Defense Nuclear Agency
Alexandria, VA 22310-3398

DNA-TR-89-273

Dosimetry for Microelectronics

Edward A. Burke
Mission Research Corporation
P. O. Box 7957
Nashua, NH 03060

May 1991

Technical Report

CONTRACT No. DNA 001-86-C-0061

Approved for public release;
distribution is unlimited.

Destroy this report when it is no longer needed. Do not return to sender.

PLEASE NOTIFY THE DEFENSE NUCLEAR AGENCY, ATTN: CSTI, 6801 TELEGRAPH ROAD, ALEXANDRIA, VA 22310-3398, IF YOUR ADDRESS IS INCORRECT, IF YOU WISH IT DELETED FROM THE DISTRIBUTION LIST, OR IF THE ADDRESSEE IS NO LONGER EMPLOYED BY YOUR ORGANIZATION.

REPORT DOCUMENTATION PAGE

Form Approved OMB No. 0704-0188

1. AGENCY USE ONLY *(Leave blank)*	2. REPORT DATE	3. REPORT TYPE AND DATES COVERED
	910501	Technical 860923 - 900223

4. TITLE AND SUBTITLE

Dosimetry for Microelectronics

5. FUNDING NUMBERS

C - DNA 001-86-C-0061
PE - 62715H
PR - RV
TA - RA
WU - DH012420

6. AUTHOR(S)

Edward A. Burke

7. PERFORMING ORGANIZATION NAME(S) AND ADDRESS(ES)

Mission Research Corporation
P.O. Box 7957
Nashua, NH 03060

8. PERFORMING ORGANIZATION REPORT NUMBER

MRC/NSH-R-89-009

9. SPONSORING/MONITORING AGENCY NAME(S) AND ADDRESS(ES)

Defense Nuclear Agency
6801 Telegraph Road
Alexandria, VA 22310-3398
RAEE/Cohn

10. SPONSORING/MONITORING AGENCY REPORT NUMBER

DNA-TR-89-273

11. SUPPLEMENTARY NOTES

This work was sponsored by the Defense Nuclear Agency under RDT&E RMC code B3230864662 RV RA 00140 25904D.

12a. DISTRIBUTION/AVAILABILITY STATEMENT

Approved for public release; distribution is unlimited.

12b. DISTRIBUTION CODE

13. ABSTRACT *(Maximum 200 words)*

Existing information on the dose enhancement effect is reviewed and current problems identified. Possible solutions are outlined. In addition, the design and use of a dual cavity ionization chamber for routine measurement of dose enhancement factors in cobalt-60 gamma test facilities is described. The enhancement factors can be derived directly from the chamber measurements without recourse to reference data that may be difficult to obtain. This relatively simple device reliably reproduced earlier results obtained by more involved equipment and procedures. Measured enhancement factors are reported for new material combinations not previously examined and compared with recent calculations.

14. SUBJECT TERMS

Dosimetry
Radiation Effects
Hardness Assurance

15. NUMBER OF PAGES

96

16. PRICE CODE

17. SECURITY CLASSIFICATION OF REPORT	18. SECURITY CLASSIFICATION OF THIS PAGE	19. SECURITY CLASSIFICATION OF ABSTRACT	20. LIMITATION OF ABSTRACT
UNCLASSIFIED	UNCLASSIFIED	UNCLASSIFIED	SAR

CLASSIFIED BY:

N/A since Unclassified

DECLASSIFY ON:
N/A since Unclassified

CONVERSION TABLE

Conversion factors for U.S. Customary to metric (SI) units of measurement.

MULTIPLY ⟶ BY ⟶ TO GET
TO GET ⟵ BY ⟵ DIVIDE

angstrom	1.000 000 X E -10	meters (m)
atmosphere (normal)	1.013 25 X E +2	kilo pascal (kPa)
bar	1.000 000 X E +2	kilo pascal (kPa)
barn	1.000 000 X E -28	meter^2 (m^2)
British thermal unit (thermochemical)	1.054 350 X E +3	joule (J)
calorie (thermochemical)	4.184 000	joule (J)
cal (thermochemical)/cm^2	4.184 000 X E -2	mega joule/m^2 (MJ/m^2)
curie	3.700 000 X E +1	giga becquerel (GBq)*
degree (angle)	1.745 329 X E -2	radian (rad)
degree Fahrenheit	τ_K=(t°f+459.67)/1.8	degree kelvin (K)
electron volt	1.602 19 X E -19	joule (J)
erg	1.000 000 X E -7	joule (J)
erg/second	1.000 000 X E -7	watt (W)
foot	3.048 000 X E -1	meter (m)
foot-pound-force	1.355 818	joule (J)
gallon (U.S. liquid)	3.785 412 X E -3	meter^3 (m^3)
inch	2.540 000 X E -2	meter (m)
jerk	1.000 000 X E +9	joule (J)
joule/kilogram (J/kg) (radiation dose absorbed)	1.000 000	Gray (Gy)**
kilotons	4.183	terajoules
kip (1000 lbf)	4.448 222 X E +3	newton (N)
kip/inch^2 (ksi)	6.894 757 X E +3	kilo pascal (kPa)
ktap	1.000 000 X E +2	newton-second/m^2 (N-s/m^2)
micron	1.000 000 X E -6	meter (m)
mil	2.540 000 X E -5	meter (m)
mile (international)	1.609 344 X E +3	meter (m)
ounce	2.834 952 X E -2	kilogram (kg)
pound-force (lbf avoirdupois)	4.448 222	newton (N)
pound-force inch	1.129 848 X E -1	newton-meter (N·m)
pound-force/inch	1.751 268 X E +2	newton/meter (N/m)
pound-force/foot^2	4.788 026 X E -2	kilo pascal (kPa)
pound-force/inch^2 (psi)	6.894 757	kilo pascal (kPa)
pound-mass (lbm avoirdupois)	4.535 924 X E -1	kilogram (kg)
pound-mass-foot^2 (moment of inertia)	4.214 011 X E -2	kilogram-meter^2 (kg·m^2)
pound-mass/foot^3	1.601 846 X E +1	kilogram/meter^3 (kg/m^3)
rad (radiation dose absorbed)	1.000 000 X E -2	Gray (Gy)**
roentgen	2.579 760 X E -4	coulomb/kilogram (C/kg)
shake	1.000 000 X E -8	second (s)
slug	1.459 390 X E +1	kilogram (kg)
torr (mm Hg, 0°C)	1.333 22 X E -1	kilo pascal (kPa)

* The becquerel (Bq) is the SI unit of radioactivity; 1 Bq = 1 event/s.
**The Gray (Gy) is the SI unit of absorbed radiation.

TABLE OF CONTENTS

TABLE OF CONTENTS (Continued)

LIST OF ILLUSTRATIONS

LIST OF ILLUSTRATIONS (Continued)

LIST OF TABLES

SECTION 1
INTRODUCTION

Standard dosimetry methods used in testing electronic piece parts in typical cobalt-60 test facilities can commonly involve errors on the order of a factor of two. It is possible in certain situations for the errors to exceed a factor of five. This can create problems when an attempt is made to correlate data collected at cobalt-60 facilities with that obtained using the recently developed low energy X-ray sources. One of the factors contributing to the problem is now commonly referred to as dose enhancement.

The basic nature of the dose enhancement phenomenon for a high atomic number material next to one of lower atomic number is illustrated by the experimental data in Figure 1. The high atomic number material is gold (or tungsten) and aluminum simulates silicon. Two curves are shown: the upper one is for the case where the gamma rays originating at the right penetrate the low atomic number aluminum before reaching the gold and the lower curve is for the case where the beam enters the gold layer first. The experimental points were obtained using ionization chambers in one case [1] and secondary emission in the other [2]. The agreement between the two techniques was excellent.

The quantity indicated on the vertical axis is the dose relative to that in a silicon equivalent dosimeter under so called electronic equilibrium conditions [3]. In fact, it can be seen that it is not until a distance of 1000 micrometers from the boundary is reached that the relative dose approaches 1.0 which is the region to which standard dosimetry applies. At the boundary, the relative dose for the upper curve exceeds a factor of two. The lower curve for the reverse beam direction starts at a value of about 1.5, rapidly drops to a value less than 0.9, and gradually rises until it reaches the equilibrium point.

The significance for modern devices is clear given the fact that critical device dimensions (e.g. gate oxides) can be less than 0.1 micrometers thick and that gold is common in device packages. Although the gold in Figure 1 was an equilibrium thickness, later observations showed that even micrometer layers produced a marked effect at cobalt-60 energies.

This boundary problem arises due to a fundamental assumption implicit in present day gamma and X-ray dosimetry methodology. The assumption is that the dimensions of the target material are large relative to the range of the energetic Compton and photoelectrons produced by the incident

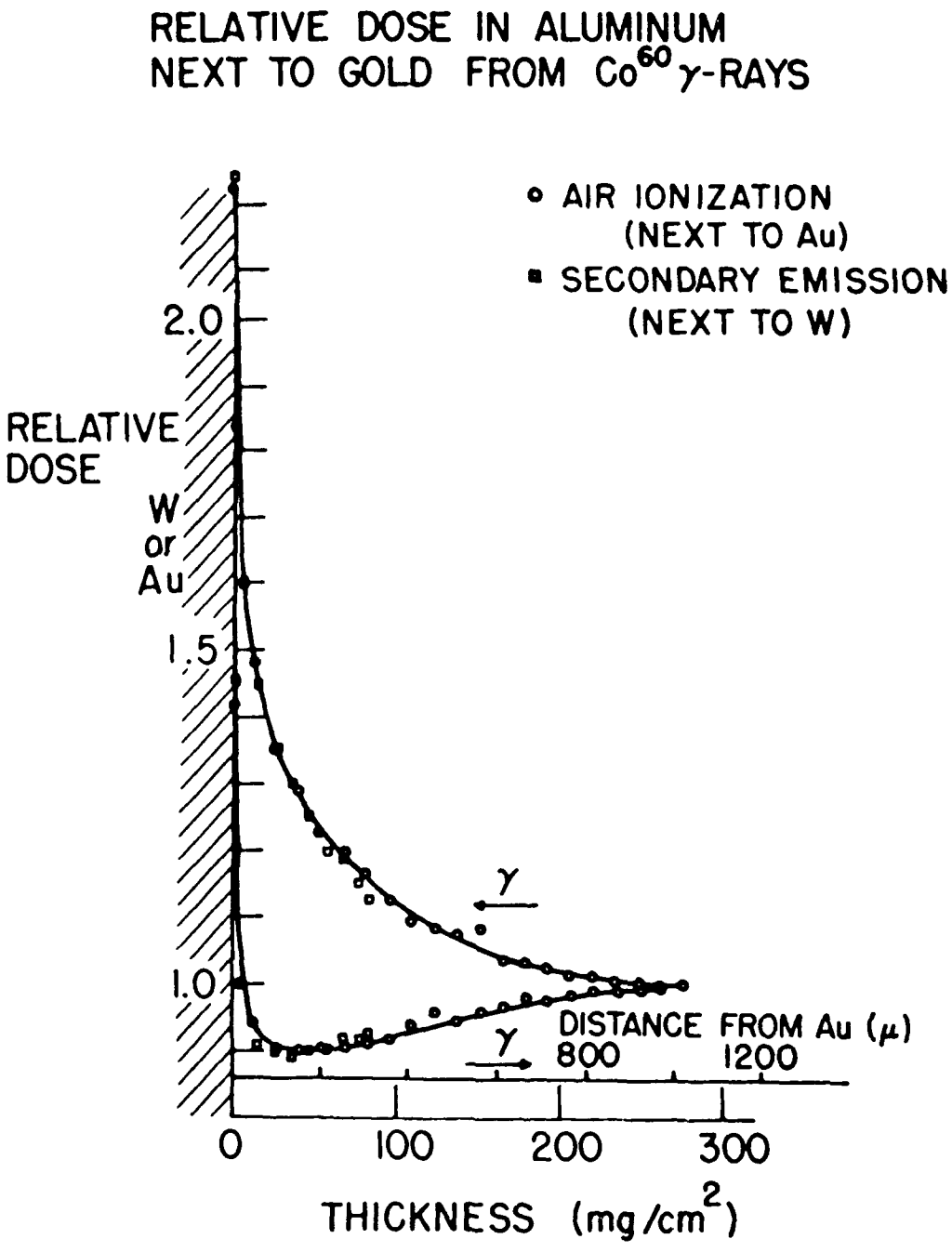

Figure 1. Air ionization and secondary emission measurements of the relative dose in aluminum next to gold as reported by Wall and Burke [1] and Frederickson and Burke [2].

high energy gamma photons Under this assumption transport of the secondary electrons away from the point where they are produced is neglected. They are assumed to impart all of their energy to the target material at the site where they are generated. This approach considerably simplifies the calculation of the absorbed energy and the interpretation of dosimeter measurements.

For modern electronic devices, however, the basic assumption that the dimensions are large relative to the range of the electrons created by the incident high energy photons is almost never justified. 1.0 MeV Compton or photoelectrons created by cobalt-60 gamma rays will have a range of about two millimeters in silicon. The result is that electrons created in materials used to package devices can easily reach sensitive parts of the device such as the gate oxide in an MOS structure. In most cases this leads to a marked enhancement in the dose which is not reflected by the conventional dosimeters.

In the first part of the report we describe the problem of dose enhancement, briefly outline early work related to it, and then review recent work that has led to our present understanding of its role in the response of microelectronic devices. The questions that remain concerning our ability to predict its role in device testing are identified.

The second section describes an ionization chamber which can be used to minimize uncertainties encountered in actual device testing in cobalt-60 test facilities. The design and performance of the chamber are described. The possibility of developing similar chambers for other types of radiation sources is discussed.

As part of the general review of factors that could lead to dosimetry problems recent work on fluctuation phenomena produced in different test environments was reviewed. In this case the problem is not that conventional dosimetry gives inaccurate information – it simply gives no information at all. Methods for calculating the magnitude of such fluctuations for X-ray and cobalt-60 environments are described and compared with experimental data in an Appendix.

SECTION 2
REVIEW OF DOSE ENHANCEMENT

2.1 EARLY WORK.

What is now commonly referred to as "Dose Enhancement" is a phenomenon that predates studies of radiation effects in semiconductor devices by decades. It is a problem that is related in a fundamental way with the measurement of the amount of energy imparted to matter by all types of radiation, but its effects are especially noticeable for X-rays and gamma rays. It occurs at boundaries between materials of different atomic number where the electron fluence is very different from that characteristic either material. The energy imparted to a low atomic number material (the absorbed dose) at a boundary with one of high atomic number is usually much greater than that in the absence of boundary effects.

This boundary or interface problem was encountered very early in studies related to the measurement of X-ray energy deposited in matter when attempts were made to relate the absorbed dose in a probe constructed of one material to that in a target of a different material. The probe was assumed small enough to produce a minimal perturbation in the dose received by the target. Early papers on this were those of W. H. Bragg (1910) [4] and L. H. Gray (1929,1936)[5]. The original theory relating the dose in the probe material to that in the target has become known as Bragg-Gray theory. In actual practice the probe consisted of a chamber with walls identical to or as close as possible to that of the target. It was filled with a gas, usually air, and the ionization produced therein taken as a measure of the absorbed energy in the gas. The theory developed by Bragg and Gray was then used to deduce the energy imparted to the surrounding target material. Later developments relating the energy deposited in the gas cavity to that in the target are referred to under the general heading of cavity theory. Excellent surveys of developments in cavity theory are available in many books such as that by Attix [6].

The essential point relative to the dose enhancement problem is that we are dealing with a situation where electron transport across an interface between different materials cannot be ignored. Cavity theory focuses on the relation between the dose in one material (the cavity gas) to that in another (the cavity wall) when the electrons responsible for the dose in both cases originate in the wall material only. An important difference between the early cavity theories and the dose enhancement problem is that cavity theory gives the average dose over a thin gas layer which may be equivalent to several

microns of solid material. Since the cavity material is a gas an average dose is the most useful way of expressing the result. In the case of the dose enhancement effect, however, the dose changes rapidly within the first few microns of a solid boundary. A detailed description of the dose as a function of distance is a much better indicator of the actual damage to the critical components of a device than an average value.

As the cavity becomes larger and the mass of gas increases electrons originating in the gas will contribute and must be taken into account. This has been the subject addressed in later developments of cavity theory by Burlin and Kearsley [7,8]. These later theories are capable of describing the absorbed dose as a function of distance from the interface. They are similar in many respects to semiempirical models developed to describe the dose enhancement effect by Burke , Chadsey and Garth [9-11] although detailed comparisons have not yet been made. In the most recent versions of the dose enhancement models, directional effects associated with beams of gamma radiation are taken into account whereas this has not yet been addressed in the cavity models.

Another area of research related to dose enhancement evolved from medical applications of radiation, especially in radiotherapy and radiobiology. The common name for the effect in this case was "transition zone dosimetry". This work was pioneered by F. W. Spiers who was especially concerned with the dose received by soft tissue next to bone [12]. The photon energys studied covered the 25 - 200 keV range reflecting the sources commonly used for radiotherapy during that period.

Work in these areas up to 1968 was reviewed by Spiers [12]. In the case of the bone marrow we have a structure roughly analogous to some of the cavity ionization chambers previously discussed i.e. a low density low atomic number material surrounded by a higher density higher atomic number matrix. It is not surprising therefore that attempts were made to calculate the dose using approaches similar to those developed for cavity chambers. However, in contrast to the early cavity theory work the bone cavities could not be assumed to be very small relative to the ranges of the electrons generated by the X-ray sources of concern. The effect of the material in the cavities was taken into account and calculations done for planar, cylindrical and spherical geometries. Other interfaces of concern included the skin and the respiratory tract. The maximum dose "enhancement factors" calculated for soft tissues in bone were about 3.5 for 35 to 50 keV X-rays.

As reported by Spiers experimental studies of these transition zone effects were carried out using chemical dosimetry (ferrous sulfate solution),biological indicators (T4 bacteriophage), and solid state dosimetry (radiation induced conductivity in polyethylene sheets). The most extensive studies were performed using ionization chamber techniques.

The later studies covered in the review by Spiers were done by Dutreix and his colleagues [13]. They included cobalt-60 and high energy bremstrahlung at energies of 11, 15 and 20 MeV. The interfaces studied involved combinations such as copper and lead next to carbon. Dose profiles were reported that qualitatively strongly resembled results later published by Wall and Burke [1] for copper and gold next to aluminum.

In summary we see that the problem associated with specifying the dose at material boundaries was recognized from the earliest days of working with X-rays. It first arose in connection with measuring dose and later in the application of X-rays to radiotherapy. Certain features of the effect at cobalt-60 photon energies were identified e.g.the sensitivity of the profile to the direction of the incident gamma rays, and the fact that the magnitude of the dose enhancement in a low atomic number material is a function of the atomic number of the material next to it. In the low energy X-ray calculations it was also found that the enhancement would go through a maximum. The material combinations studied, however, were not those of prime interest in the case of effects on semiconductor devices and the computational models involved assumptions that were not valid for the semiconductor case. Consequently, most of this early work had relatively little impact upon the developments that were to begin in the area of radiation effects on semiconductor devices.

2.2 DOSE ENHANCEMENT IN SEMICONDUCTOR DEVICES.

2.2.1 Early Studies.

The first recorded concern over the dose to silicon near a layer of gold or other materials of high atomic number appears in two papers presented at the 1969 IEEE Nuclear and Space Radiation Effects Conference. These results were not published in the December issue of the IEEE Transactions on Nuclear Science but do appear in the Summaries of Papers which were distributed to attendees at that time.

One of these papers was presented by K. W. Dolan and J. L. Wirth of Sandia Laboratories and was entitled "Non-Local Energy Deposition in Silicon by Energetic Electrons" [14]. The specific problem addressed was the poor correlation between theory and experiment found in the experimental determination of photocurrents induced by low energy flash X-ray machines. It was found that devices exposed to flash X-ray machines yielded photocurrents which exceeded predicted values by a factor of two or more while those obtained with high energy (20 MeV) Linacs were in essentially exact agreement with theory. It had been assumed that the discrepancies were due to dosimetry errors but the source had not been identified. It was suspected that photoelectrons injected into the silicon from gold eutectic bonds were a possible source of the enhanced photocurrents. Silicon PN diodes with gold or aluminum backings were irradiated with a 600 kVp flash X-ray machine. The diode with the gold foil backing was found to yield a pulse four times larger than the diode with the aluminum backing. This is essentially the same factor that would be derived from later Monte Carlo calculations. Pulse height analysis experiments using a PIN detector indicated that photoelectrons from the gold were responsible.

The other paper by L. S. Mims and R. A. Williams of Autonetics was entitled "Effects of Packaging on Radiation-Induced Responses" [15]. This paper also focussed on the generation of photocurrents due to both gold eutectic bonding and from gold plated transistor covers. The study involved both measurements and calculations. They concluded that the enhanced dose could be an order of magnitude greater than that in the absence of gold. They estimated an enhancement factor as high as 57 for 50 keV X-rays on a gold-silicon interface. This is about a factor of two higher than given by later Monte Carlo results.

2.2.2 Multicavity Ionization Chamber Measurements.

A 1970 paper entitled "Gamma Dose Distributions At and Near the Interface of Different Materials" by Wall and Burke was the first paper published on dose enhancement in the IEEE Transactions on Nuclear Science [1]. The motivation for this work evolved from previous studies of low energy secondary electron emission yields from various materials bombarded with gamma rays and high energy electron beams. It had been found that the yields were proportional to the energy deposited in surface layers of the bombarded materials. The problem of determining the surface dose in various circumstances was investigated and the available information found to be incomplete. It was decided to measure the dose experimentally using multicavity ionization chambers which were based upon modified secondary emission vacuum chambers. An exploded view of chamber construction is shown in Figure 2.

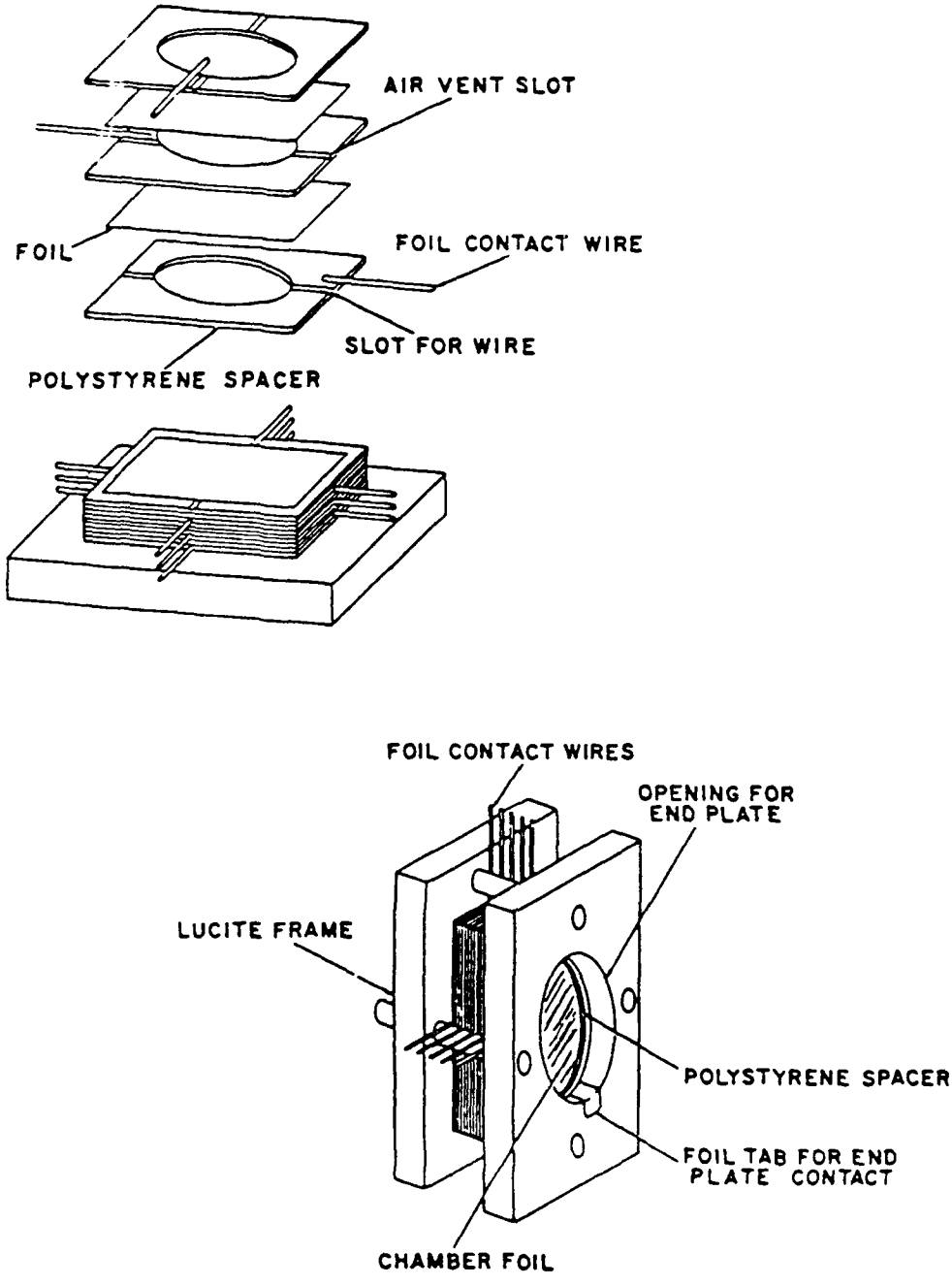

Figure 2. Original multicavity ionization chamber.

The experimental studies reported in this paper involved the determination of dose profiles in aluminum and gold next to beryllium, carbon, magnesium, copper, and molybdenum. Hybrid configurations were also studied involving aluminum sandwiched between gold and carbon. The dependence of the profile shape upon the direction of the gamma beam was clearly evident in these studies. The material combinations were different but qualitatively resembled and supported the results reported earlier by Dutreix et al. The maximum measured enhancement was found to be 2.2 in aluminum next to gold when the gamma beam approached the interface from the aluminum side.

The study of the dose enhancement effect was considerably expanded by Burke et al., in 1971 [1,2,16,17]. Since the ionization chamber measurements had shown that the dose changed rapidly with distance near an irradiated interface it was decided to obtain more detailed measurements in this zone. A new parallel plate aluminum ionization chamber was constructed with variable foil thicknesses instead of the single foil thickness used in the original chamber. The new chamber had 3.4 mg/cm^2 foils near the interface (0.0025 cm or 0.5 mils) graded up to 20 mg/cm^2 (0.05 cm or 10 mils) near the chamber center. The new chamber permitted accurate empirical fits to the data as well as the determination of the effects of thin films of gold on the dose distribution in aluminum.

2.2.3 Early Calculations of Dose Enhancement.

As soon as it became clear that significant dose perturbations occurred at gold-silicon interfaces the question arose as to the photon energy where the effect would become largest. Consequently, at the same time the measurements were being made in mid 1970 Sherman [18] undertook calculations of dose enhancement factors at a gold-silicon interface as a function of photon energy. As a point of departure he used the cavity theories and transition zone calculations of Spiers [12], Charlton [19], and other early workers. Extensive modifications were necessary because the high atomic number materials of interest in semiconductor effects were not included in the early transition zone analyses. At this time it was suspected that at low X-ray energies dose perturbations might also occur at silicon-silicon dioxide interfaces even though these materials are ordinarily considered identical for energy deposition by energetic photons. The results of these calculations are shown in Figure 3. The gure shows that the maximum dose enhancement factor was predicted to be 30 at 120 keV and 10 at 20 keV. The calculations extended only to 150 keV because of the strong directional effect of the early models. It was interesting to find that at energies below 15 keV the dose in SiO_2 would be enhance by a factor of 1.5. We will compare these factors with later analytical and Monte carlo results. They are the first known calculations of these quantities.

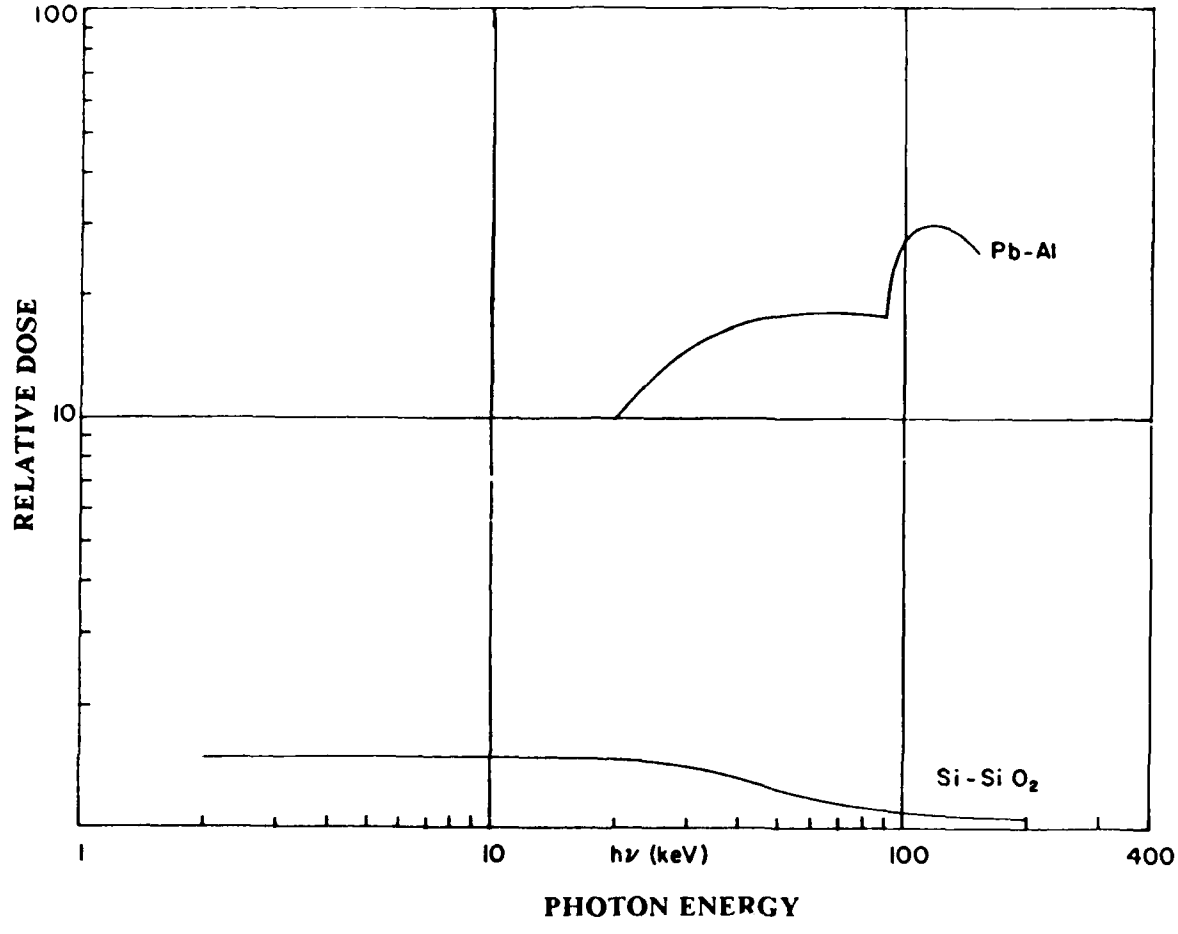

Figure 3. Calculation of the dose enhancement factor with photon energy for Pb-Al and Si-SiO_2 from Sherman [18].

2.2.4 Empirical Fits to the Dose Enhancement Data.

Empirical fits to the data were found by Wall [17] to follow an expression of the form

$$D = 1.0 + Ae^{-ax} + Be^{-bx} + Ce^{cx} \qquad (2.1)$$

where

D = the dose relative to an all aluminum chamber

x = thickness of aluminum in mg/cm^2

A,B,C,a,b,c are constants derived from fits to the data

The constants for various wall materials are shown in Tables 1 and 2.

2.2.5 Dose Enhancement Produced by Thin Gold Films.

Experimental studies of the effect of thin gold films are shown in Figure 4. As can be seen only a few microns of thickness has a readily detectable effect.

The thin gold film measurements clearly showed that the dose enhancement problem was important for gold thicknesses comparable to those encountered in device packages even at cobalt-60 gamma energies.

2.2.6 Fundamental Assumptions Underlying the Ionization Measurements.

The multicavity ionization chambers had yielded a large amount of information concerning the nature of the dose enhancement effect but the interpretation of the information in terms of dose raised some questions. It had been assumed that the air ionization observed in the experiments was simply proportional to the dose delivered to the adjacent cavity walls. The assumption is valid if that portion of the secondary electron energy spectrum responsible for the ionization does not change markedly in the vicinity of the interface (the transition zone). The reason for this assumption rested in part on the fact that the modified cavity theory devised by Burlin was based on a similar assumption (e.g. see Burlin in Attix [3] pp 365 et seq.). His arguments for this were based upon extensive experimental information derived from studying energy deposition by beta rays that had been reported by many investigators.

Table 1. Dose profiles in aluminum next to various elements.

Element	A	B	C	a	b	c
Higher Atomic Number Facing the Source						
Be	-0.159	0.0751	0	0.0213	0.137	0
Cu	-0.183	0.192	0	0.0094	0.0749	0
Mo	-0.356	0.426	0	0.0138	0.0450	0
Ag	-0.332	0.211	0.320	0.0114	0.0341	0.251
Cd	-0.299	0.206	0	0.0081	0.0827	0
Au	-0.262	0.255	0.284	0.0097	0.0408	0.351
Lower Atomic Number Facing the Source						
Be	0.283	-0.0836	0	0.0122	0.325	0
C	0.119	0	0	0.0079	0	0
Cu	0.204	0.293	0	0.0172	0.334	0
Mo	0.294	0.312	0	0.0173	0.200	0
Ag	0.311	0.288	0	0.0158	0.216	0
Cd	0.306	0.202	0	0.0167	0.115	0
Au	0.526	0.231	0.249	0.0144	0.0998	0.346

NOTE: Carbon does not appear in the first part of the table due to repeated irregularities in the data, the cause of which was never determined.

Table 2. Dose profiles in aluminum next to gold films.

Film Thickness (microns)	A	B	C	a	b	c
Gold Facing the Source						
25.4	-0.203	0.290	0.404	0.0104	0.0442	0.320
12.7	-0.193	0.265	0.437	0.0131	0.0311	0.258
6.35	-0.0596	0.465	0	0.0122	0.124	0
1.40	-0.0316	0.0539	0.329	0.00734	0.044	0.312
0.65	-0.0277	0.221	0	0.0136	0.220	0
Aluminum Facing the Source						
25.4	0.410	0.417	0	0.015	0.158	0
12.7	0.260	0.552	0	0.0195	0.256	0
6.35	0.198	0.418	0	0.0214	0.212	0
1.40	0.0596	0.276	0	0.0215	0.216	0
0.65	0.199	0	0	0.183	0	0

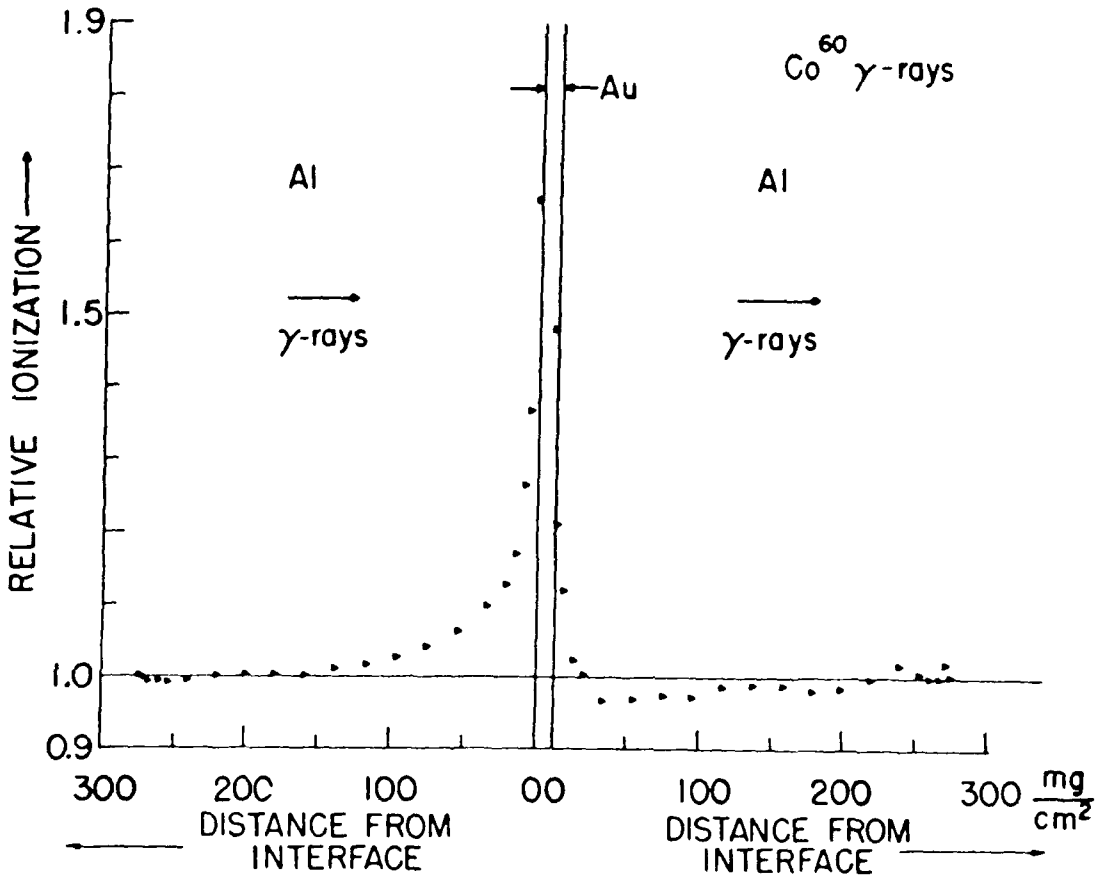

Figure 4. **Energy deposition for a thin gold layer (6 microns) between equilibrium thicknesses of aluminum [1].**

2.2.7 Secondary Emission Measurements of Dose Enhancement.

The fact that Burlin found that the assumption of a stable electron energy spectrum led to calculations which were in excellent agreement with cavity chamber experiments lent further support for its adoption in the multicavity measurements of dose enhancement. As a further check, however, it was decided to attempt to reproduce the ion chamber results using a completely different physical mechanism [2]. It had previously been shown that the low energy (<50 eV) electron yield from an irradiated surface was proportional to absorbed dose. The secondary emission mechanism, therefore, provided an opportunity to check the ionization measurements. It was found that the secondary emission measurements agreed within a few percent with the previous ionization measurements reinforcing the interpretation of the latter as an indicator of relative dose.

2.2.8 Dose Enhancement in Multiple Layers.

A series of measurements had been taken of dose profiles in aluminum sandwiched between two different materials e.g. gold and beryllium. It was found that the results for the two interfaces in such cases could be reproduced by a superposition of the results from experiments on single interfaces [20]. For example the Au-Al-C profile could be obtained by combining the Au-Al-Al and the Al-Al-C results. Figure 5 illustrates the method. To be more explicit for an aluminum layer of thickness T sandwiched between gold and carbon the dose enhancement factor would be given by

$$D(Au/Al/C)x = D(Au/Al)x + D(Al/C)T-x - 1.0 \qquad (2.2)$$

where

D(Au/Al/C)x	Enhancement ratio at x for the sandwich structure.
D(Au/Al)x	Enhancement ratio at x for Au/Al
D(Al/C)T-x	Ratio at T-x for Al/C

The limits of applicability for the superposition approach has not been determined but it was found to apply down to aluminum thicknesses equal to one half the range of the most energetic electrons produced. For the photoelectrons created by cobalt-60 one half the range in aluminum amounts to about 0.1 cm.

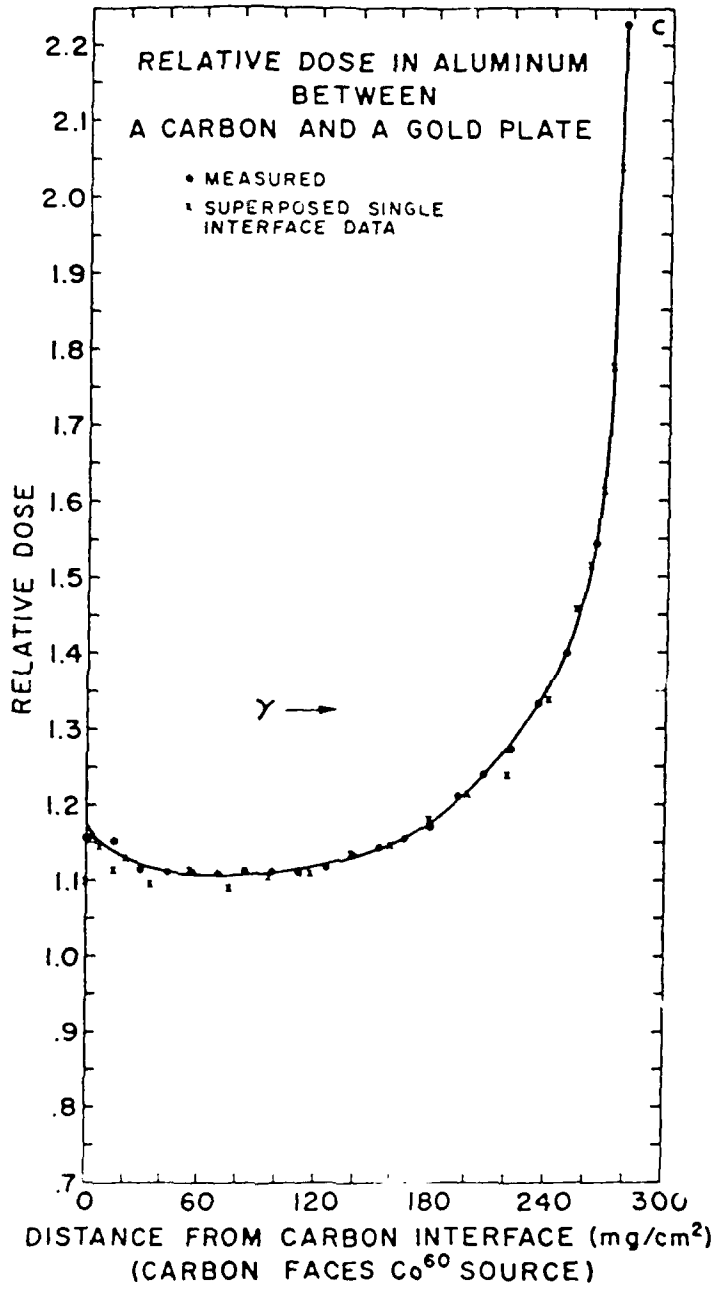

Figure 5. Relative dose distribution in aluminum between carbon and gold from Wall and Burke [20].

2.2.9 Early Comparisons with Monte Carlo Calculations.

The first comparison of the multicavity chamber results with Monte Carlo calculations was carried out by M. J. Berger [21]. The calculations were done assuming a broad beam of cobalt-60 gamma photons. The results obtained were in good agreement with the multicavity measurements for the case where the beam entered the aluminum first but showed a marked departure from the calculated results for the opposite direction as shown in Figure 6. The reason for this discrepancy was not clear at the time.

In addition to the above studies a Monte Carlo electron transport code that had been developed to calculate photo-Compton current distributions for SGEMP applications was modified to derive dose distributions at interfaces of dissimilar materials [22]. It was used to calculate profiles at planar gold-aluminum interfaces irradiated by 300 kVp and 1000 kVp bremsstrahlung spectra, a cobalt-60 spectrum, and 30, 100, and 200 keV monochromatic X-rays. The X-ray spectra are shown in Figures 7 and 8. Comparisons with the unpublished data of Wall are given in Figures 9 and 10. The agreement with experimental results for the X-ray spectra is very good.

Comparisons with the cobalt-60 data show discrepancies similar to those found by Berger. They are most noticeable for the case where the photons enter the gold first as can be seen in Figure 11. Based upon preliminary calculations and measurements it was estimated that in the original experiment by Wall and Burke, Compton scatter in the collimator employed, and from the source itself, contaminated the gamma beam with low energy photons. It was estimated that 3% of the incident energy was in this low energy spectrum with a peak at about 200 keV. When this component was added to the original calculation the overall results were within 10% of those measured as seen in Figure 12.

2.2.10 Comparisons of Device Response to Ionization Chamber Results.

Although reasonable agreement had been found between ionization chamber readings and Monte Carlo calculations (after allowing for the presence of Compton scattered photons) it was decided to determine if the ion chamber data could actually be used to predict device response. Accordingly the response of N/P solar cells was measured as a function of the atomic number of the medium adjacent to the cell for two directions of the cobalt-60 beam [23]. The dose profile used to calculate the minority carrier generation was that measured with the multicavity chamber. The measured short circuit current represents an average over the cell. The measured and calculated currents agreed within a few percent.

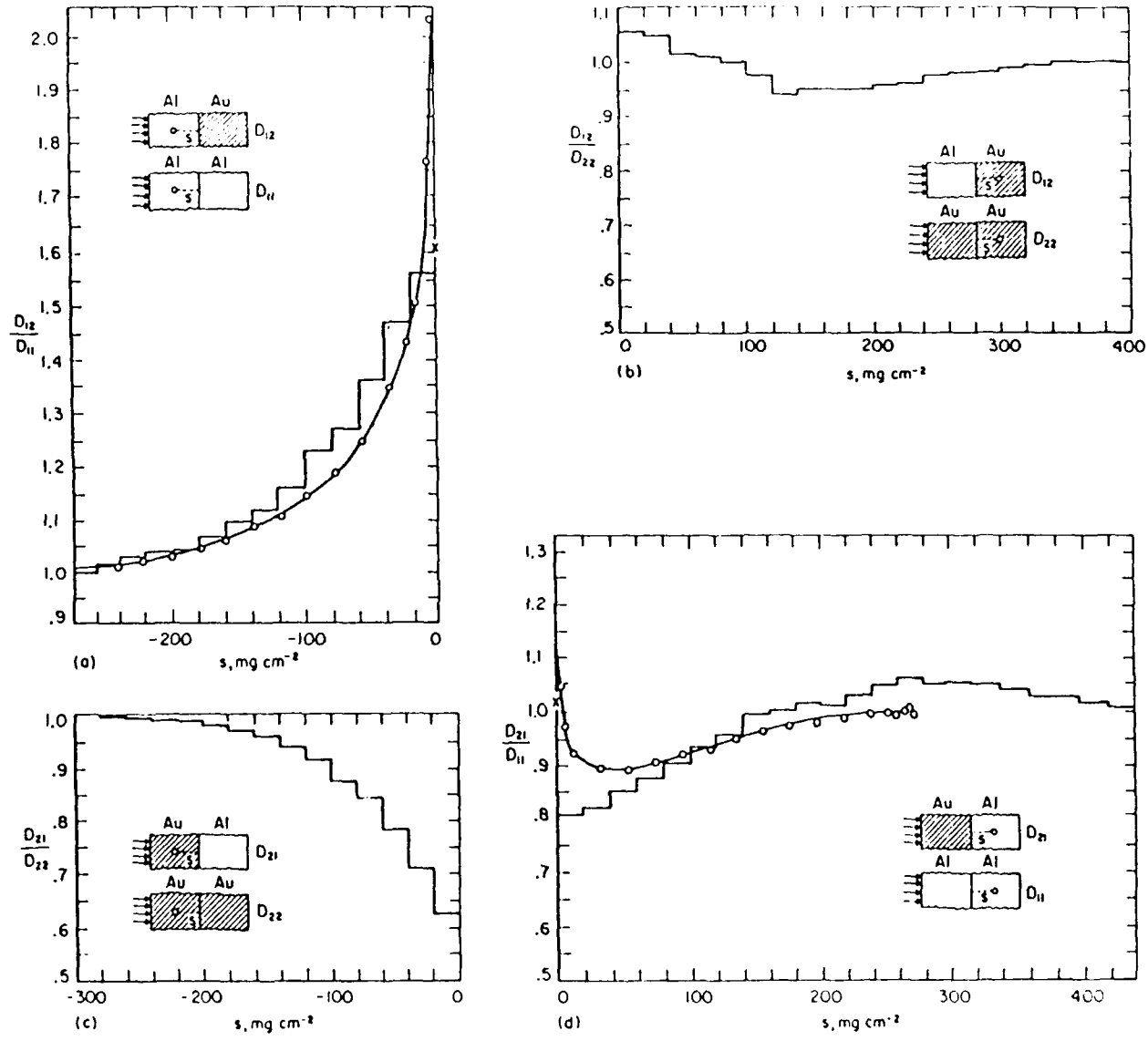

Figure 6. **Relative dose for aluminum-gold targets. Histograms are calculated by Berger [21] and data points from Wall and Burke [1].**

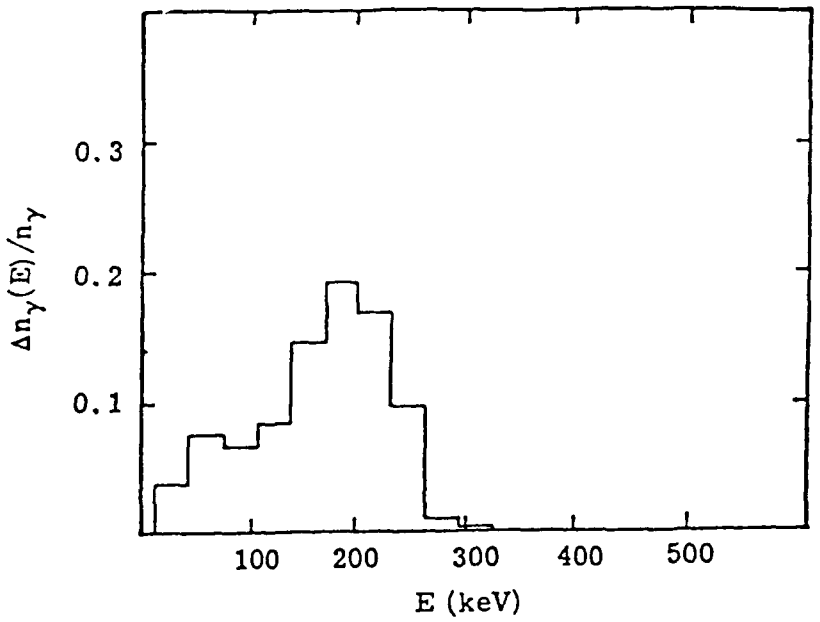

Figure 7. 300 kVp X-ray spectrum used for dose profiles shown in Figure 8 from Chadsey [22].

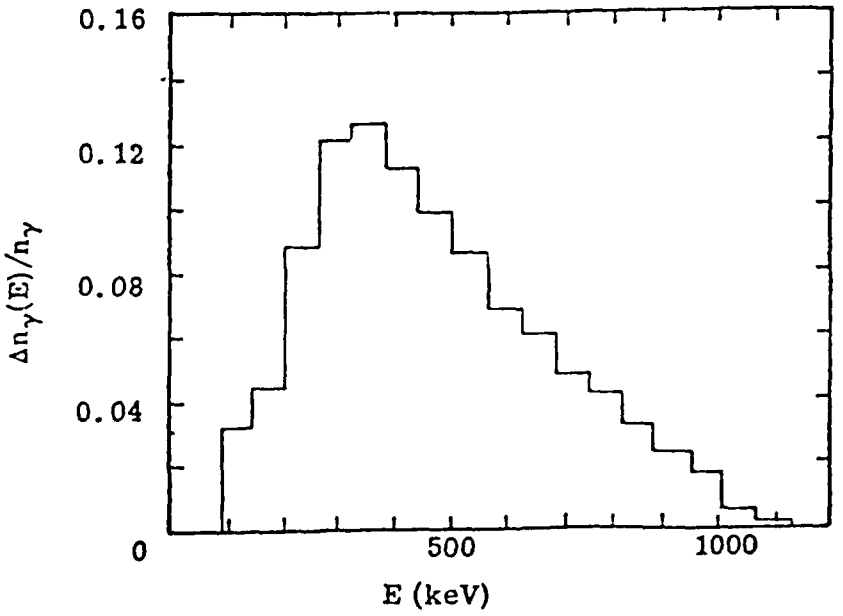

Figure 8. 1000 kVp X-ray spectrum used for dose profiles shown in Figure 9 from Chadsey [22].

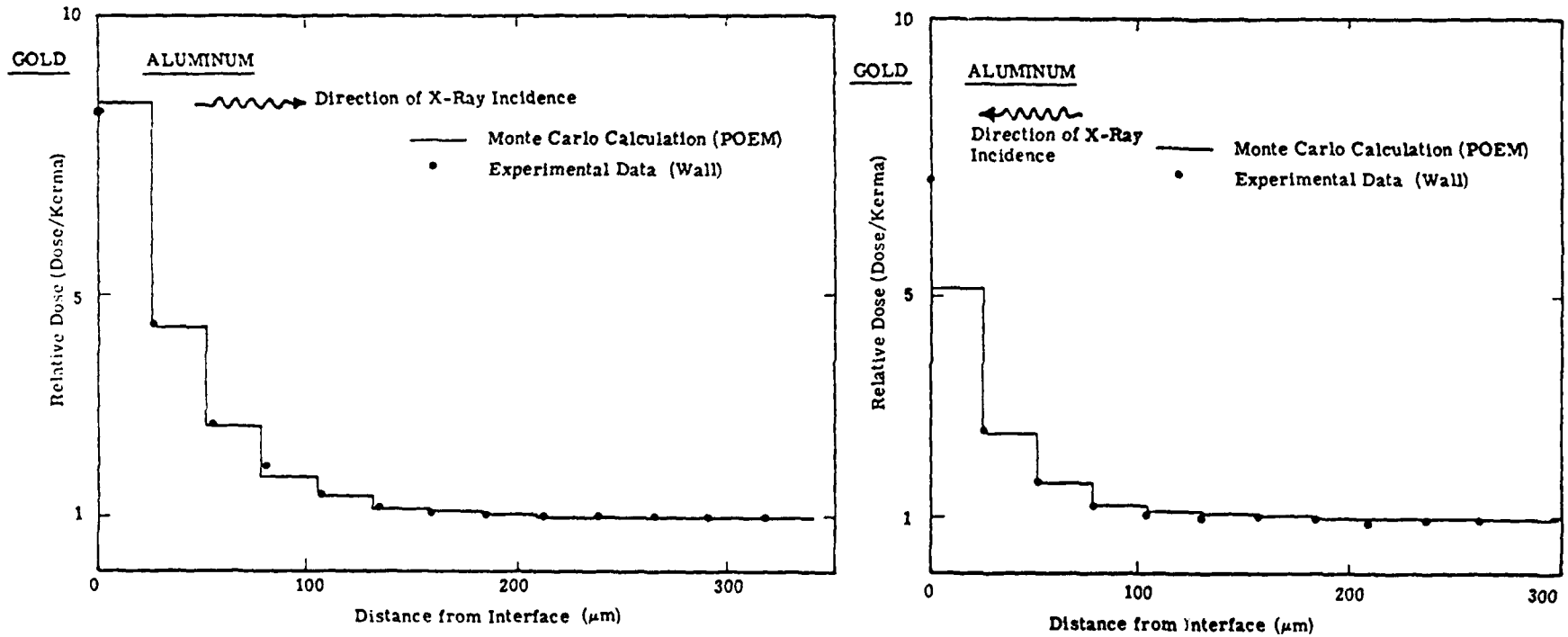

Figure 9. **Experimental relative dose profiles for 300 kVp X-rays compared with Monte Carlo calculations.**

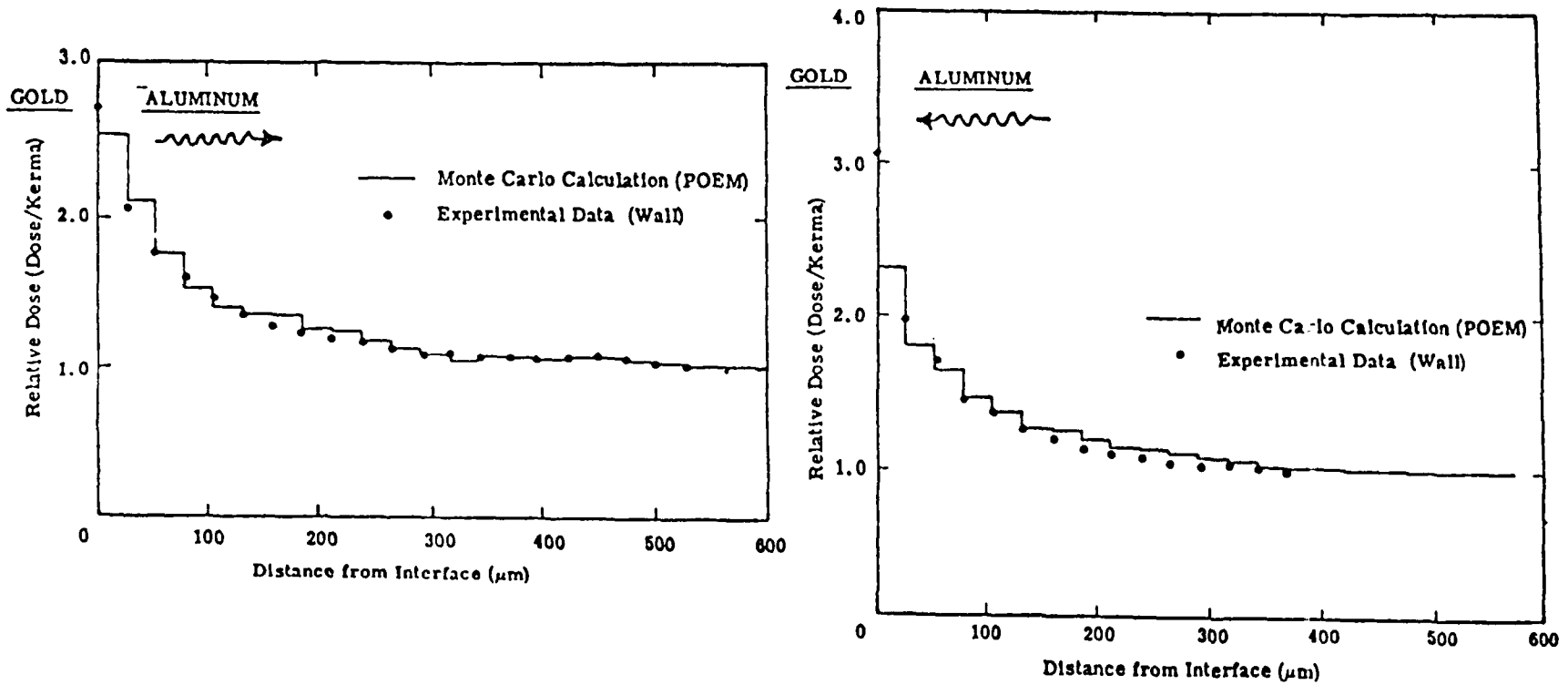

Figure 10. Experimental relative dose profiles for 1000 kVp X-rays compared with Monte Carlo calculations.

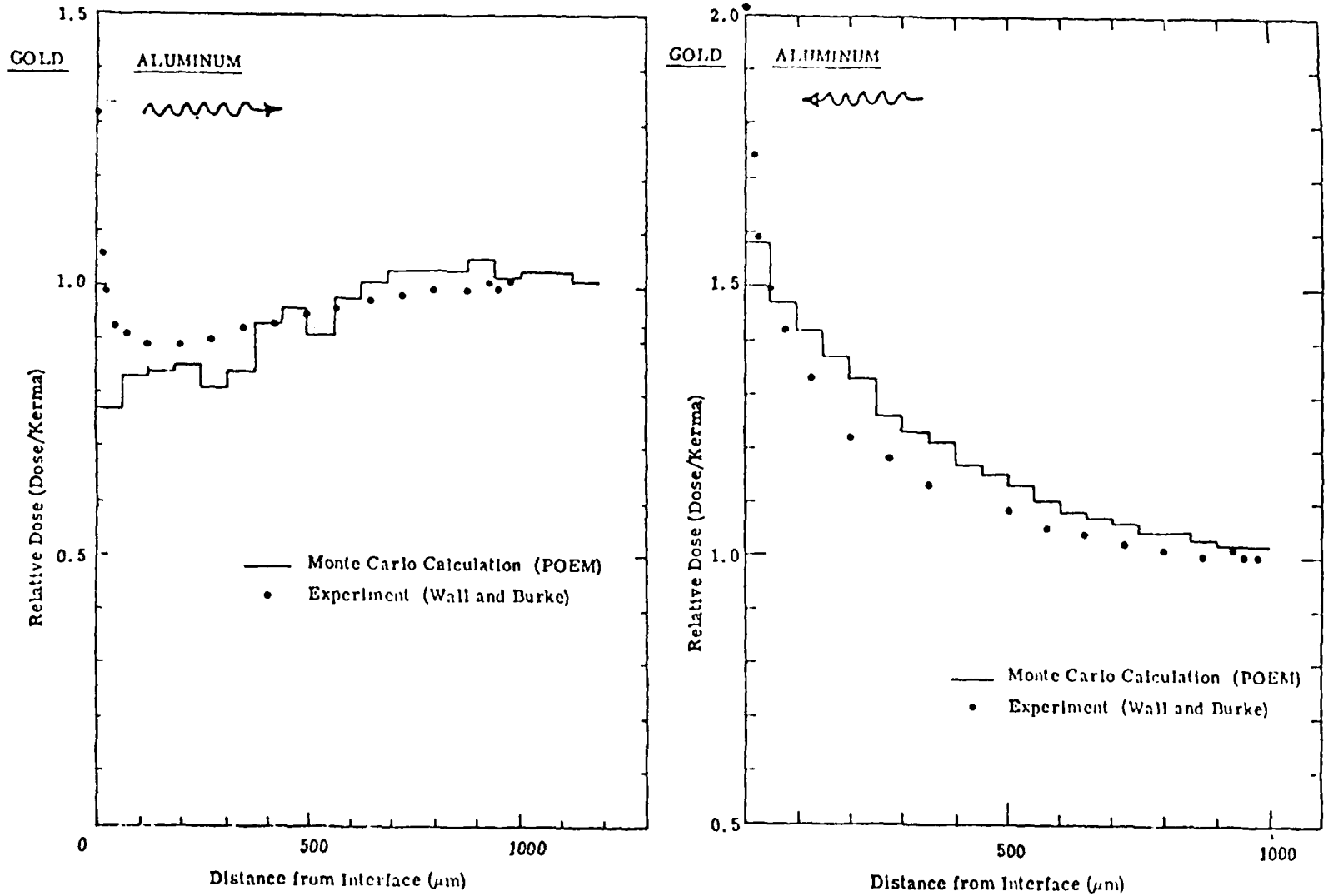

Figure 11. Experimental relative dose profiles for cobalt-60 compared with Monte Carlo calculations.

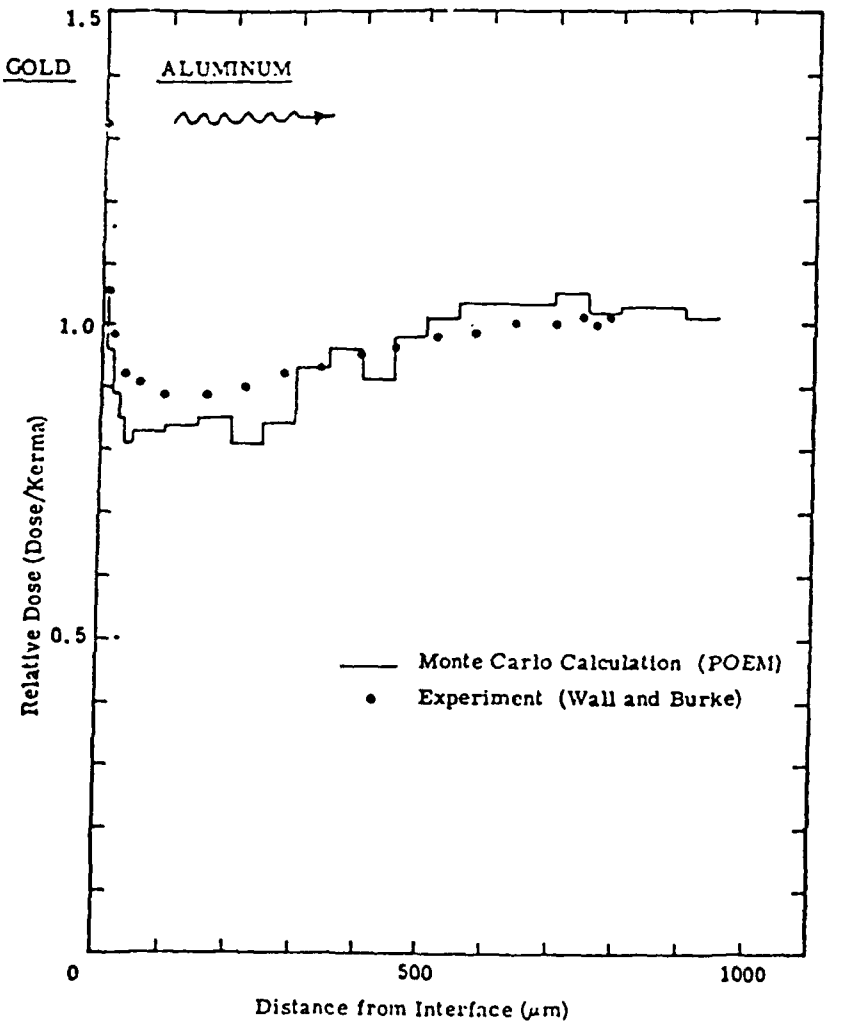

Figure 12. Relative dose in aluminum next to gold when 3% of the incident gamma energy consists of scattered photons [22].

2.2.11 Gamma Ray Induced Charge Buildup in Insulators.

The dose enhancement effect is closely related to the phenomenon of charge buildup in insulators adjacent to materials of different atomic number. The charge buildup results from the rapid change in the fast electron current as it crosses the interface and moves into the dielectric material. As we know the dose in this transition region also changes rapidly. The radiation induced conductivity which is directly related to the dose rate is strongly affected by the dose profile. A paper published in 1974 described an analytical method for calculating the number current, energy current, and energy deposition at the photon irradiated interface between different materials [24]. Dose profiles were not given but the dose enhancement factor in silicon at the gold silicon interface was given for photon energies between 0.01 and 10 MeV as shown in Figure 13. This is the first reported calculation of the dose enhancement factor as a function of incident photon energy above 200 keV. The magnitude and position of the peak enhancement agree with the early results of Sherman [18].

2.2.12 Dependence of Dose Enhancement on Gamma Beam Direction.

All of the measurements and calculations discussed up to this point were for a beam direction normal to the irradiated interface. Monte Carlo calculations were carried out for photon energies of 30 keV, 100 keV, and 200 keV at angles of photon incidence varying from 0 to 85 degrees both for photons incidence on the gold and on the aluminum [22]. The results of the calculations for the lowest and highest energies are shown in Figures 14 and 15. Experimental studies [25] using CaF2:Mn-teflon thermoluminescent dosimeters (TLD's) confirmed the main result of the Monte Carlo calculations, namely, that the largest effect occurred at normal incidence. Additional experiments on angular dependence were carried out by Long and Swant [26]. They again showed that for a gold-silicon interface the maximum enhancement factors for 0.3, 6.0, and 10 MVp X-rays occurred for photons incident at 0 and 180 degrees. As a result most studies since that time have focussed upon the case of normal incidence. The Monte Carlo code employed in these and many later studies was described in a 1975 report [27]. The essential finding in all of these experimental and theoretical studies was that the dose enhancement effect was always greater for normal incidence of the photons.

2.2.13 Dose Enhancement in Different Types of Devices.

Up until 1974 the number of studies on actual device types had not been extensive. In that year an extensive study was reported for an MOS (metal-oxide-semiconductor) transistor, a bipolar transistor, a linear integrated circuit, and a PIN (P-Intrinsic-N) diode [28]. Tests were carried out

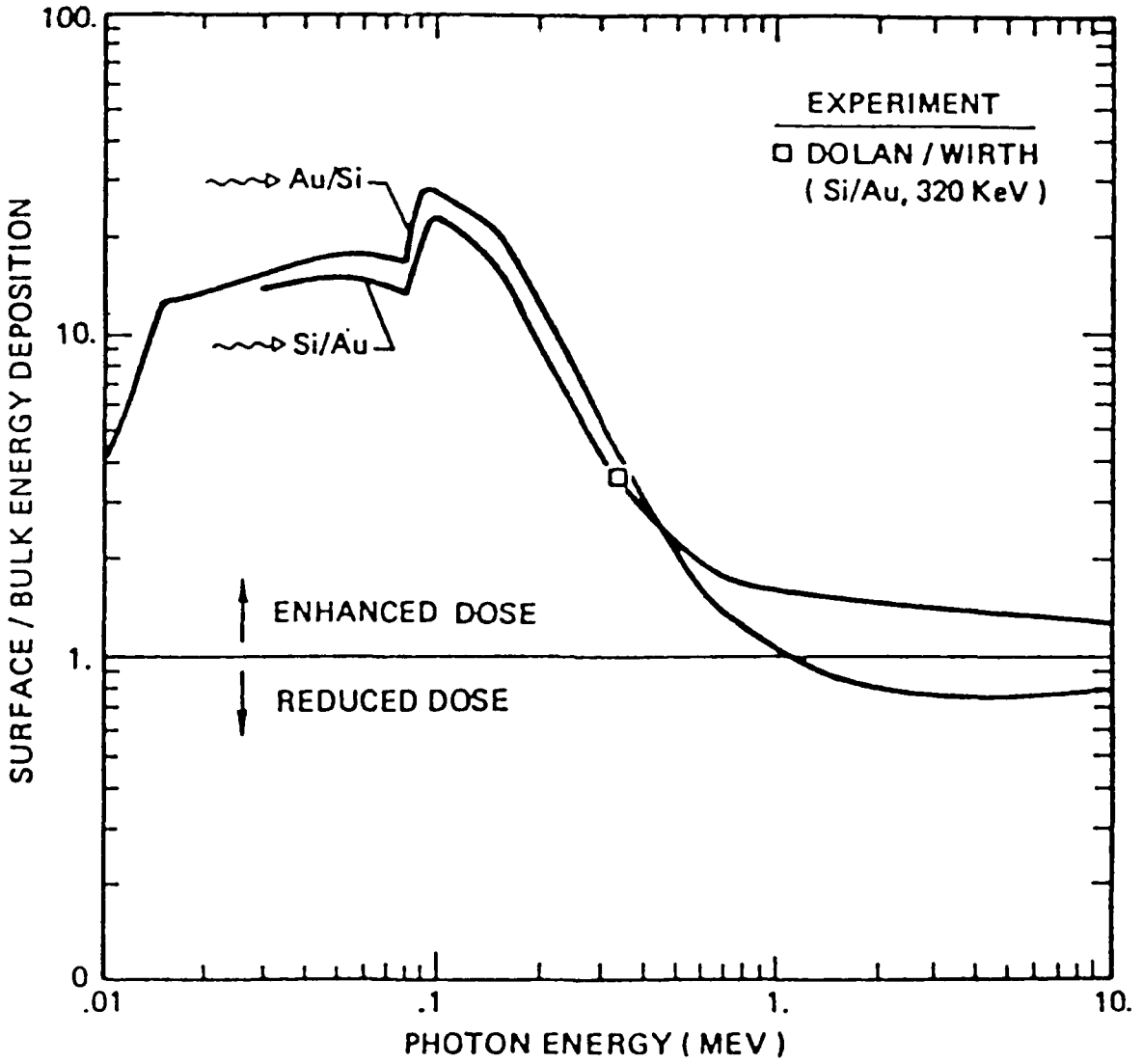

Figure 13. Dose enhancement factor for silicon next to gold versus photon energy from Dellin et al [24]. The term surface/bulk is the dose enhancement factor.

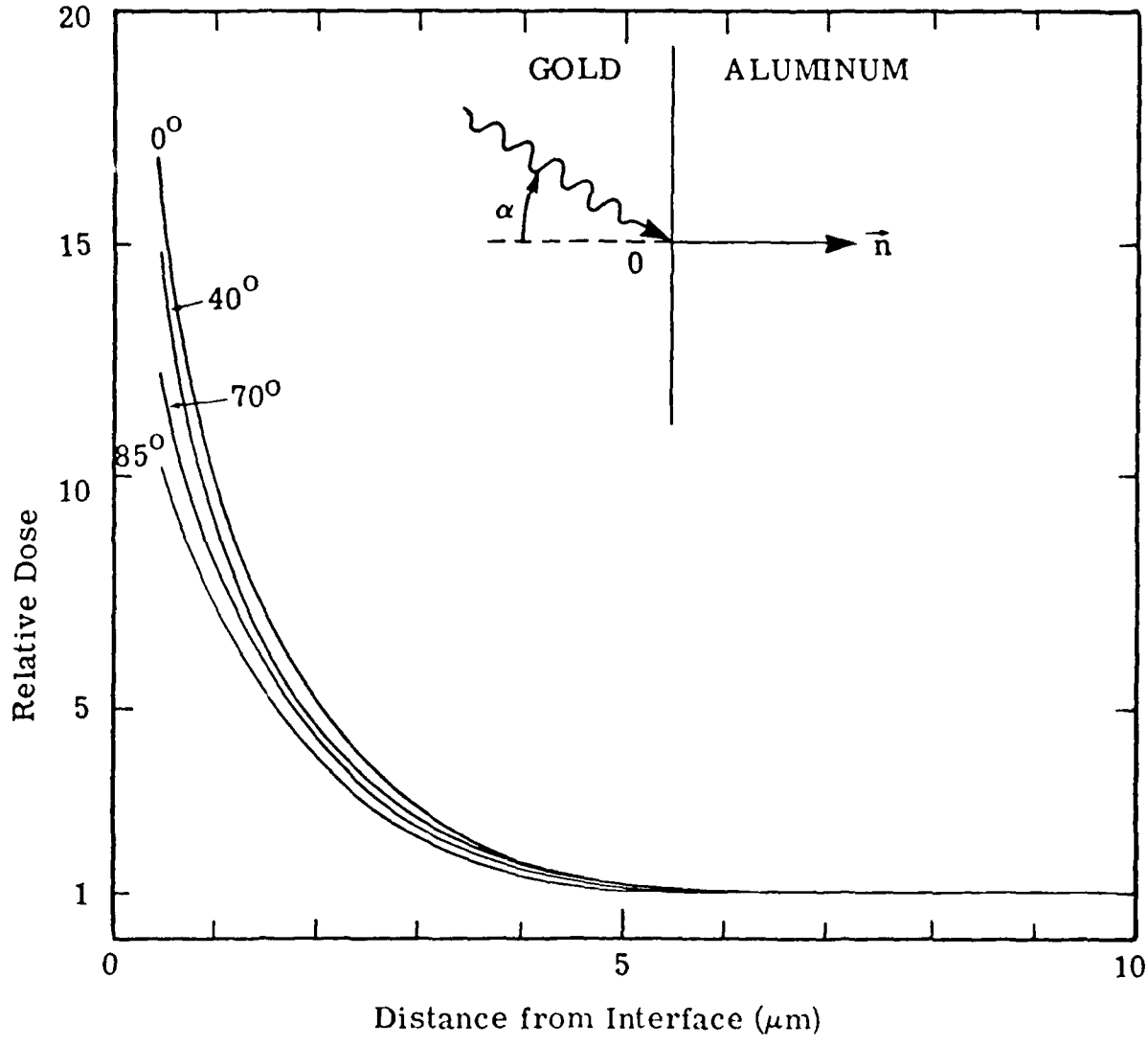

Figure 14. Relative dose enhancement in aluminum next to gold vs angle of photon incidence for 30 keV X-rays from [22].

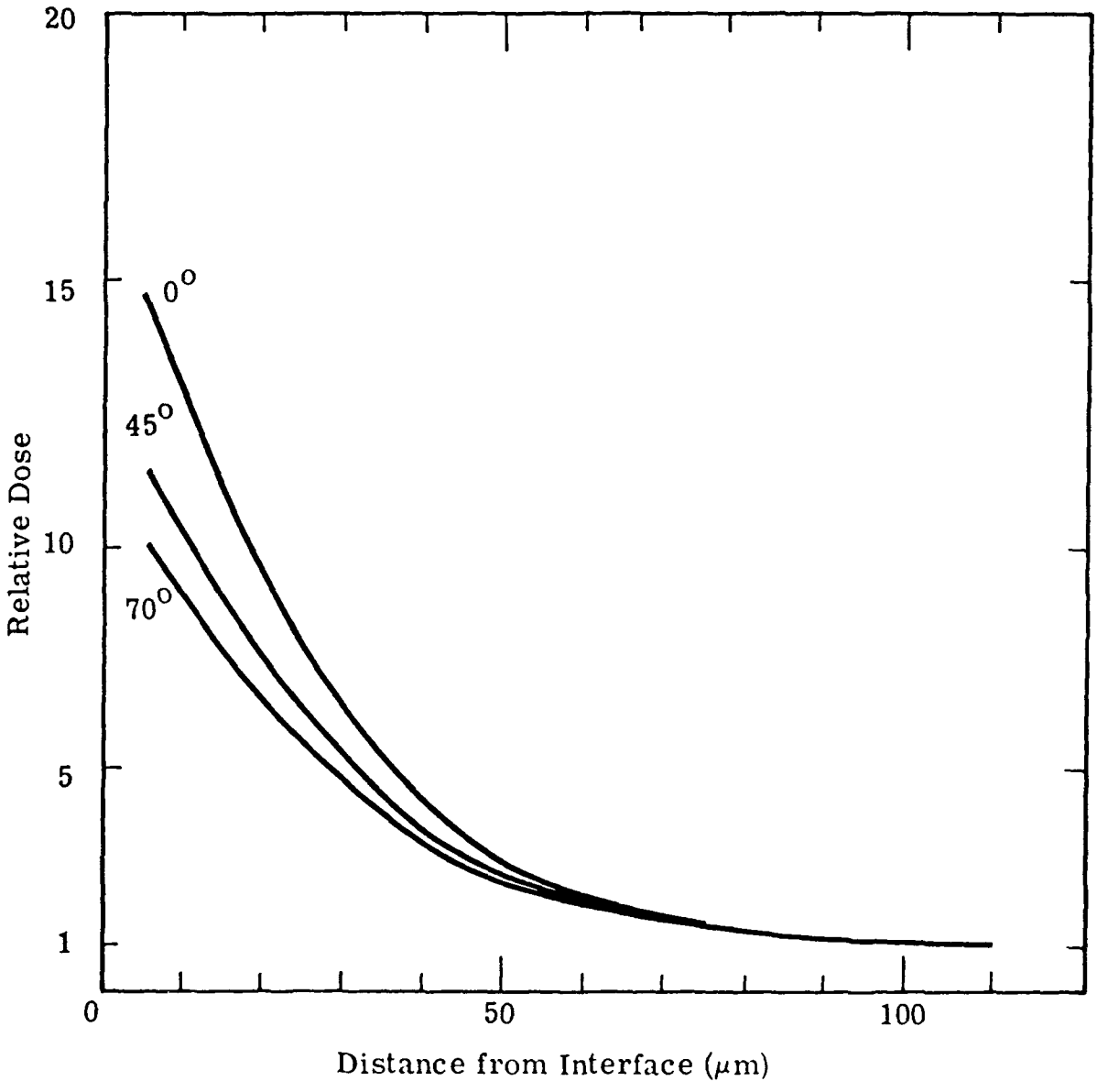

Figure 15. Relative dose enhancement in aluminum next to gold vs angle of photon incidence for 200 keV X-rays from [22].

with 300 kVp flash X-ray, 2 MVp flash X-ray and 10 Mev Linac bremsstrahlung. The enhancement effects of gold, copper, ceramic, aluminum and mylar were examined. A condensed tabulation of the results is given in Table 3. The enhancement factors ranged from 17 for the MOS device exposed to 300 kVp X-rays to 1.0 for the PIN diode exposed to 10 MVp bremsstrahlung.

Table 3. Experimental dose enhancement factors for several types of devices.

Device	300 Kevp Fx Brem	2 Mevp Fx Brem	10 Mevp Linac Brem	6 MeV Linac Elect
Transistor	6.0	2.6	1.6	1.3
Pin Diode	1.6	1.5	1.0	1.2
IC	4.2	2.2	---	1.2
MOS	17.0	3.8	---	---
TLD	2.9	1.3	---	---

Additional device tests were reported in 1975 on the photocurrents generated in bipolar switching transistors exposed to low average (100 keV) and high average (600 keV) energies [29]. The devices were packaged in Kovar and Kovar/gold TO-5 cans. The SANDYL Monte Carlo code was used to calculate the dose profiles through the sensitive regions of the devices and the photocurrents for the different packages calculated. The calculations yielded results which were in excellent agreement with experiment. The maximum dose enhancement factor measured and calculated was about 5.0.

In 1982 a paper by Long, Millward, and Wallace [30] outlined an engineering methodology which accounted for the primary dose enhancement effects in generic semiconductor devices/packages. Dose enhancement factors were computed for key conditions and provided in tabular form. Both total dose and transient response were considered. Radiation sources considered included flash X-rays, LINAC's and cobalt-60. A number of specific examples were provided. Additional details were given in a technical report published in 1983 [31].

Extensive studies of dose enhancement in flash X-ray environments were reported in 1985 [32]. This involved the use of the CMOS IC detectors previously employed to study enhancement in cobalt-60 tests. In this case the theoretical estimates were a factor of two higher than the experimental results. Attempts to identify the source of the discrepancy were unsucessful.

2.2.14 Parametric Monte Carlo Calculations.

The Monte Carlo approach was believed to be the most reliable (but time consuming) method for calculating dose perturbation at boundaries. Calculations of dose enhancement as a function of photon energy up to 1975 had involved only analytical or semipirical methods. Accordingly, the POEM Monte Carlo code was used to calculate enhancement factors as a function of photon energy between 10 an 2000 keV [33]. This was done for gold next to silicon and gold next to polyethylene. In view of the rapid change of the dose with distance from the boundary, the calculations were done at distances of 0, 2, 5, 10, and 30 microns from the boundary. The results are shown in Figures 16-19. The data for the gold-silicon case agree very well with the previous analytic and semi empirical calulations. The enhancement factor for polyethylene next to gold reached a value of 400 at photon energies below 50 keV.

2.2.15 Comparisons Between Calculations.

In 1976 a number of further developments were made in the area of calculation. In the paper by Dellin and MacCallum the analytical QICK E4 code was compared with the Monte Carlo codes POEM, SANDYL, and ZTRAN [34]. Comparisons were made for dose profiles at the gold-silicon interface for photon energies of 50, 320, and 2000 keV. In general the agreement was very good.

As a result of the extensive parametric calculations carried out with POEM the preceeding year a semi-empirical model was developed which permitted rapid calculations for cases where Monte Carlo results were unavailable [9-11]. This model was later simplified and extended by Chadsey in 1978 to enable the calculation of dose profiles as well as the dose immediately at the interface. The agreement with the POEM code was very good.

2.2.16 Calculations at Energies Below 10 keV.

Up to 1979 all of the theoretical dose enhancement calculations had been done for energies above 10 keV except for the results of Sherman for the silicon-silicon dioxide interface. A series of calculations over the 0.1 to 10 keV energy range were done using the semi-empirical model [35]. The materials studied included SiO_2 next to gold, silicon, and aluminum. The results agreed with the earlier Sherman calculation where the two could be compared. An analytical model based upon extensive

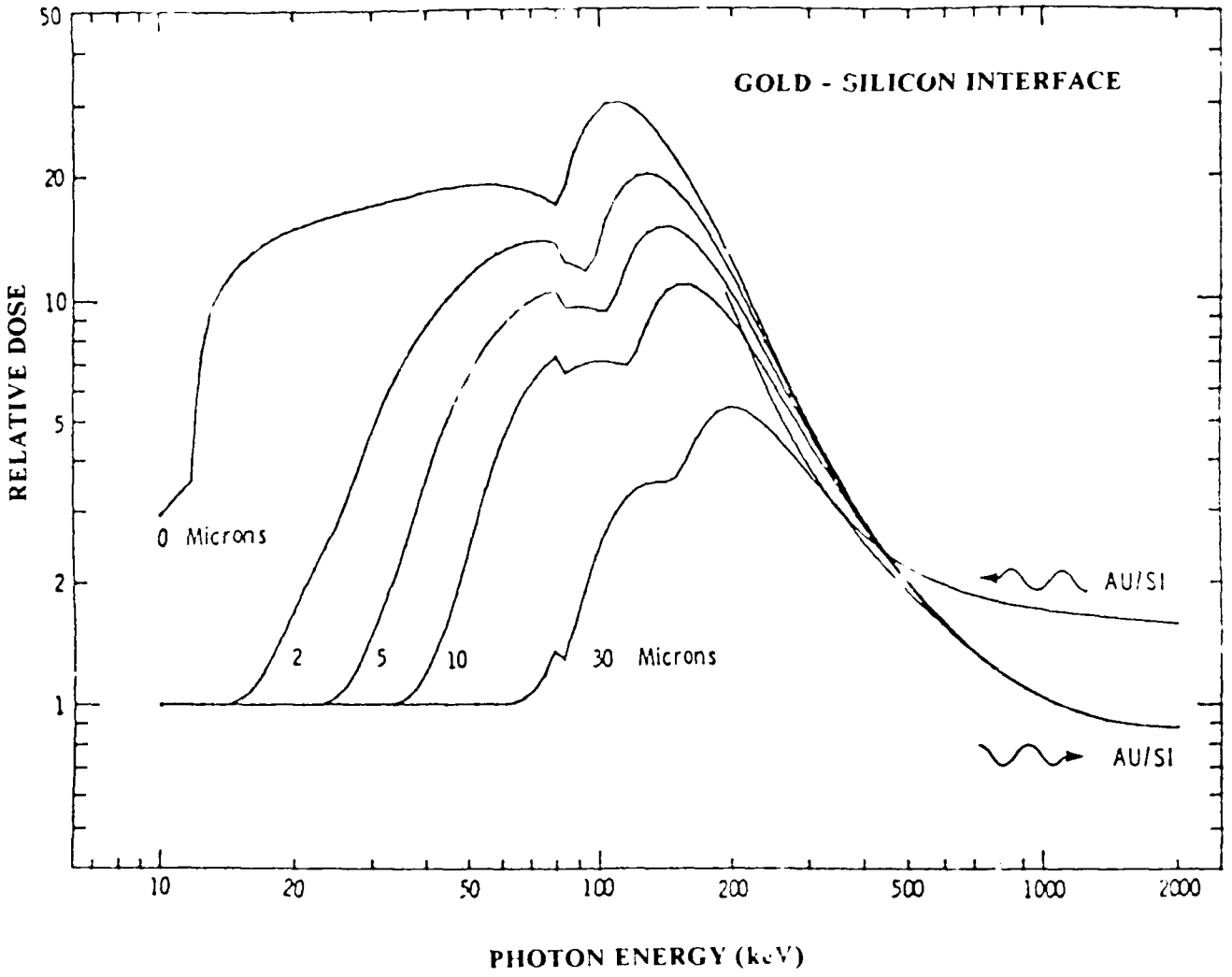

Figure 16. Dose enhancement factor for silicon next to gold versus photon energy from Chadsey et al [33].

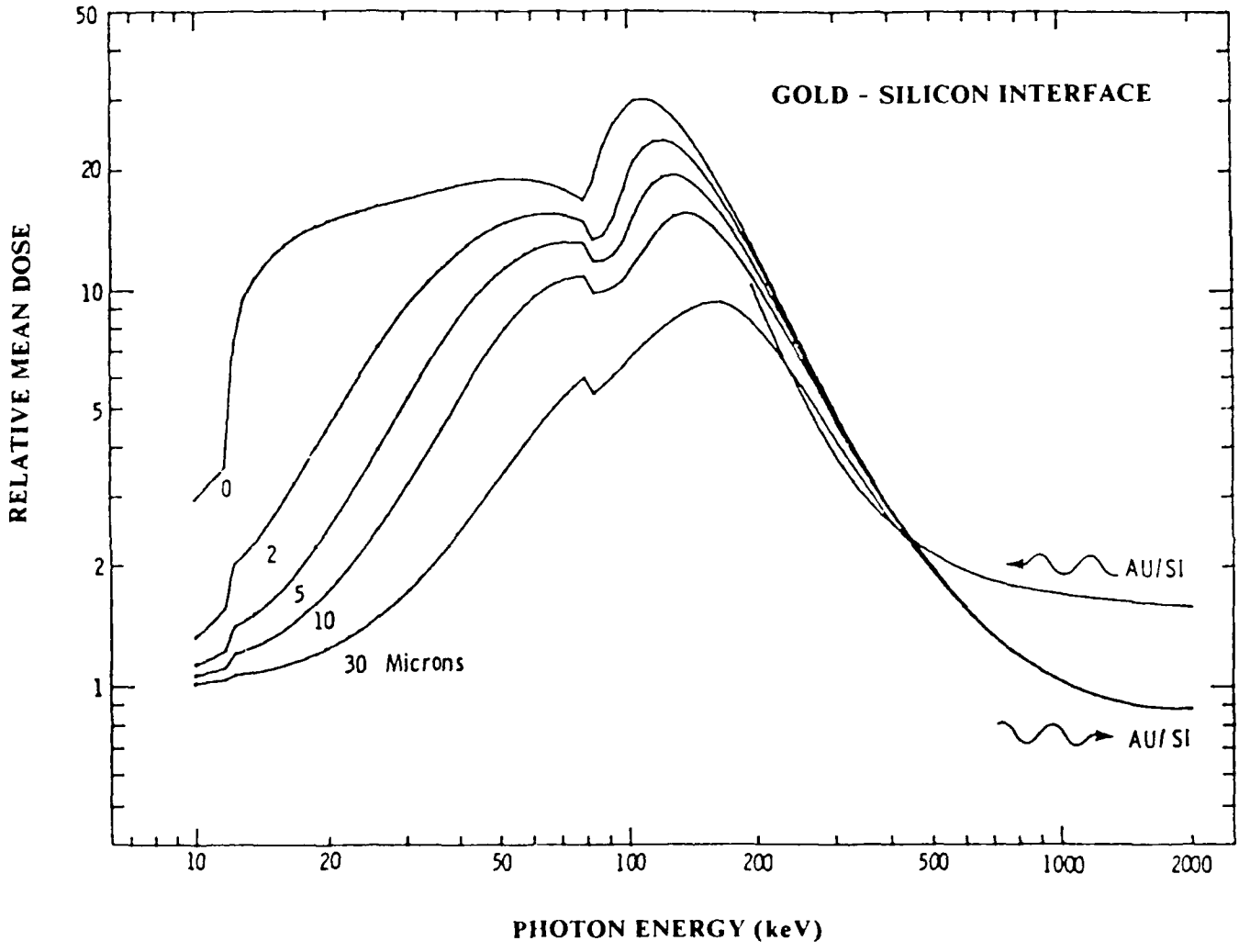

Figure 17. Mean dose enhancement factor for silicon next to gold versus photon energy from Chadsey et al [33].

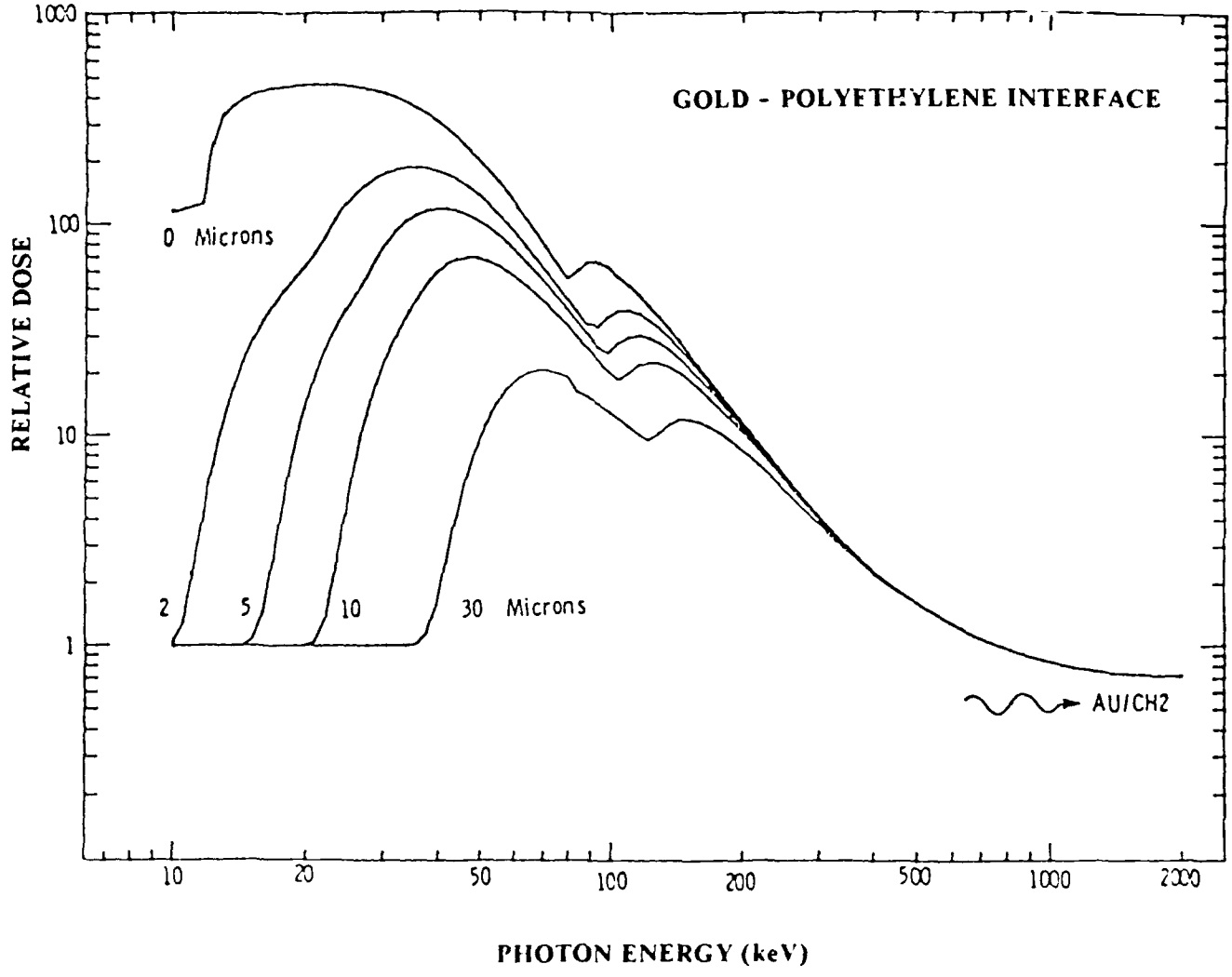

Figure 18. Dose enhancement factor for polyethylene next to gold versus photon energy from Chadsey et al [33].

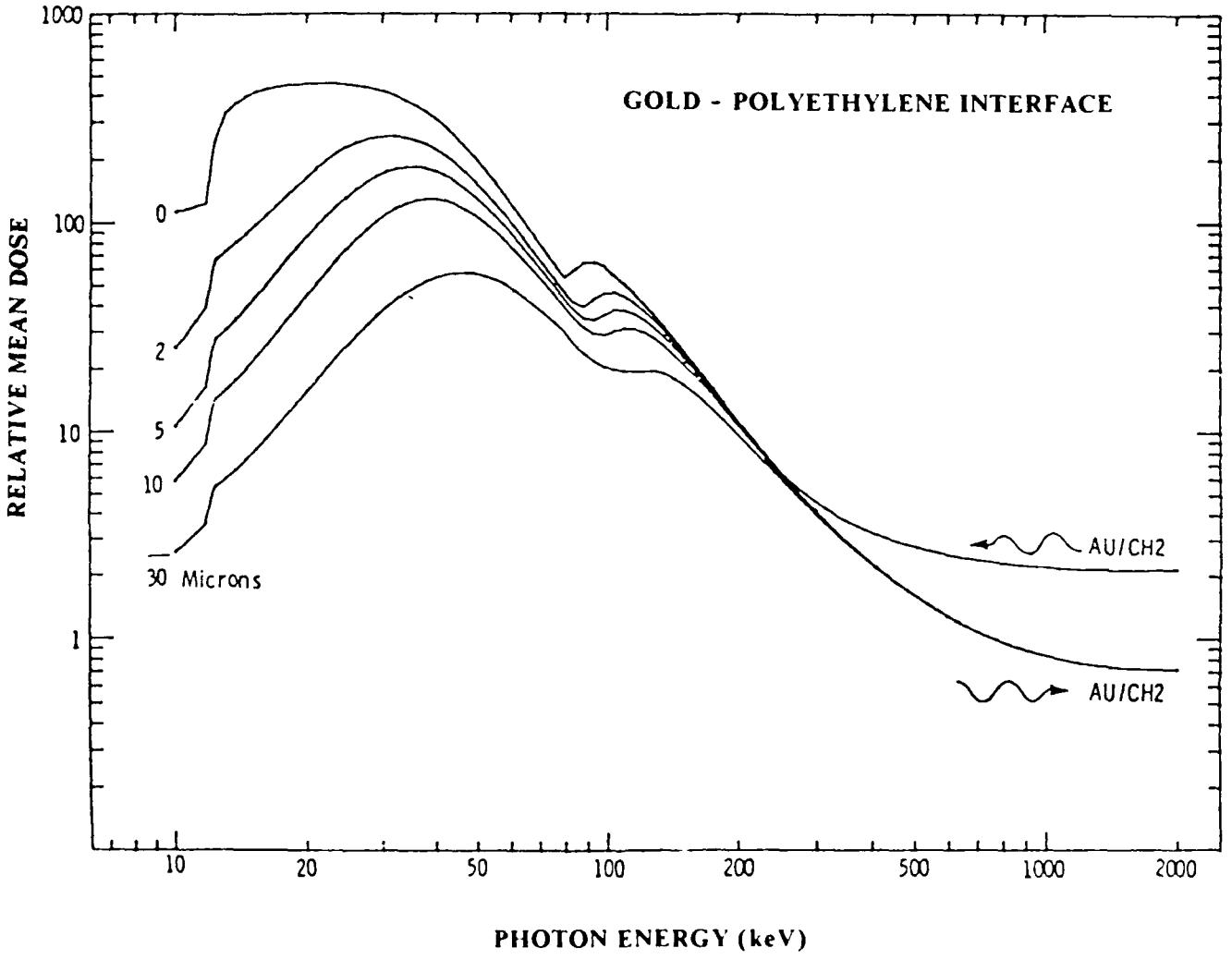

Figure 19. Mean dose enhancement factor for polyethlylene next to gold versus photon energy from Chadsey et al [33].

earlier work on X-ray production and X ray analysis was applied to the low energy X-ray range by Brown in the following year [36]. Many of the cases treated in [35] were examined with substantially the same results.

2.2.17 The Effects of Scattered Radiation on Dose Enhancement.

As previously indicated the original multicavity ion chamber data collected at a cobalt-60 source did not agree well with Monte Carlo calculations near the boundary between dissimilar materials. It was suspected that the primary reason for the disagreement was the presence of Compton scattered radiation generated in the source material and the collimator used in the original experiments. In the early work only approximate methods were used to estimate the amount and spectrum of the scatter. The availability of a Monte Carlo code for calculating the scattered spectrum permitted a more quantitative assessment. Not surprisingly the calculated scattered spectrum brought experiment and theory into much better agreement.

The importance of scattered radiation in a "typical" cobalt-60 radiation cell precipitated the question of how variable the results could be due to changes in the conditions for photon scattering. This lead to a series of experiments involving the measurement of dose enhancement with ion chambers where the chamber surroundings were varied by using paraffin wax to generate low energy scatter and lead for supression of the scattered component [37]. It was found that aluminum and paraffin wax had much the same effect. Twenty centimeters of paraffin wax increased the enhancement factor at the gold aluminum interface from 2.0 to 3.0. In the same year Brown and Dozier reported on a method for reducing enhancement errors by using a lead filter [38]. Additional details on a filter which can be used routinely in device testing was provided in a 1984 paper by Dozier and Brown. This approach has since been incorporated into an ASTM standard [39].

The scattered radiation problem in cobalt-60 test cells was further explored using the Monte Carlo code MCNP in two separate papers [40,41]. This included concrete rooms, water wells, and the Gammacell 220. The results indicated that the the scattered component in concrete rooms varied widely ranging from 38 to 63% of the total number of photons incident on the target. Approximately 50% of the photons in the Gammacell 220 are scattered. The NBS water well also showed large variability in the scatter amounting to 40 to 60%.

Further studies of the effect of scattered radiaton in MOS devices exposed in typical gamma test facilities was reported by Kelly et al in 1983 [42]. Calculations were performed for devices in gold-Kovar packages and compared with measurements. The measured values of dose enhancement factors were 1.5 to 1.6 compared with 1.3 to 1.6 for the best calculations. With a lead filter the enhancement was reduced to less than 1.2.

2.2.18 Dose Enhancement in Devices: X-Rays vs Cobalt-60.

Low energy X-ray sources (10 keV) have been proposed as alternatives to cobalt-60 for device testing [43]. It is essential in this case to be able to correlate results obtained with these two sources. In 1983 two papers identified dose enhancement and the field dependence of recombination as mechanisms which could show significant differences in the two environments. Oldham and McGarrity [44] measured the dose enhancement in silicon dioxide next to aluminum and found excellent agreement with calculations of Dozier and Brown. The latter [45] carried out calculations for tungsten silicide and found enhancement factors as large as 5.5 .

In 1985 two papers compared results obtained with X-ray and cobalt-60 sources. The conclusions reached were different. In one case [46] it was reported that correction factors had to be applied for dose enhancement and electron-hole recombination in order for the results obtained with the two sources to agree. The other study [47] reported good agreement between the two sources without applying enhancement or recombination corrections.

In 1986 a number of papers reported further information concerning the problem of correlating X-ray and cobalt-60 results [48-50]. From the point of view of the present report the most relevant finding was that the TIGER series Monte Carlo codes commonly used for dose enhancement calculations had failed to yield agreement with any of the experimental results! Part of this discrepancy was attributed to a lack of accurate information concerning the incident X-ray spectrum and its interaction with the structures of the target. This was analogous to the problem encountered with cobalt-60 sources in the early studies of the dose enhancement effect. Far more serious was the suggestion that the way the basic physics of the electron transport process was treated in these codes might be at fault - especially for electron energies below 10 keV. Factors mentioned included: discrepancies in comparisons of low energy electron backscatter with code predictions, failure of the assumptions underlying the condensed history approach, and the fact that electrons with energy below 1 keV are not tracked in the transport process. The condensed history approach enables a marked reduction in computer time by treating groups of collisions using multiple scattering theory rather than following each collision. The interested

reader should refer to Berger's article [3]. Two papers presented at the same time furnished support for considering the low energy cutoff problem [51,52]. In [51] it was shown that for thin films of SiO_2 (less than 0.05 microns), transport of electrons with energies less than 10 eV was important. It was shown that lowering the electron cutoff energy from 9-eV to 3.6-eV reduced the dose enhancement factor in SiO_2 from 1.45 to 1.30. The effect was larger in a film of oxide half as thick falling from 1.50 to 1.35. The importance of low energy electrons in the production of holes was clearly brought out by the work of Brown [52]. Several of the studies presented at the time emphasized that more direct correlation between sources could be achieved by using a measure of damage, e.g. hole generation, rather than dose.

Work on the anomalous X-ray cobalt-60 results continued through 1987. Some of the discrepancies previously reported were removed but the oxide field dependence could not be accounted for theoretically. The general problem of correlating effects produced by different photon environments became more complex with the report of problems in the medium-energy X-ray dose enhancing environment [53]. A broad bremsstrahlung spectrum was used with average X-ray photon energies of 60, 105, and 140 keV. The temperature, gate bias, oxide thickness, and spectrum dependencies of the relative enhanced response (RER) of CMOS devices was measured and compared to TIGERp code predictions of the expected dose enhancement. Satisfactory agreement was not found for cases of practical systems interest. These included thick oxides at low fields, thin oxides and diodes. Reasons for the disagreement were not clear.

In 1988 further extensive studies of the role of dose enhancement were reported [54,55]. The response of MOS capacitors to low and medium energy X-ray irradiation was reported as a function of gate material, oxide thickness, and electric field. Two discrete ordinate codes and the Monte Carlo TIGERp code were used to calculate dose enhancement effects. The dose predictions were combined with the most recent recombination data to arrive at theoretical predictions of device response. Good agreement was found at fields of 1 MV/cm for both aluminum and tantalum silicide gates. At higher and lower fields, however, the disagreement increased significantly and exceeded a factor of 2 at fields below 0.1 MV/cm. The general conclusion was that the discrete ordinates and Monte Carlo codes provide very reasonable estimates of dose enhancement in MOS structures. The difficulty of translating the dose predictions into enhanced device response remained most likely due to uncertainties in electron hole-recombination and other field dependent factors. If better than factor of two estimates are required, the authors concluded that carefully controlled experiments remain the most reliable way of determining the effect of dose enhancement on response of MOS circuits.

2.3 ENHANCEMENT REVIEW SUMMARY.

The first step in correlating the effects of different types of radiations or the effects at different incident energies is to determine by measurement and/or calculation the energy imparted to the sensitive regions of the target. As mentioned at the beginning of this review microelectronic devices have dimensions such that the basic assumptions upon which standard dosimetry theory and practice are based do not hold. In particular the standard theory assumes that the photo and Compton electrons produced by energetic photons have ranges which are small relative to critical dimensions (e.g. gate oxide thickness) of the device under test. Under such a constraint boundary effects are not important. This condition is usually addressed under the heading of "charged particle equilibrium". Of practical importance are cases where the energy imparted to a target significantly exceeds that derived from dosimeter measurements. It turns out that the most common semiconductor material, silicon, is frequently found in the presence of higher atomic number elements. The higher cross section of such elements for the production of photoelectrons leads to the injection of these electrons into the adjacent silicon leading to an effect which has come to be known as "dose enhancement". The response of the target may or may not be simply related to the energy deposition. The focus of concern here has been on how well we can estimate the dose and not on the connection between the dose and the response of the target device.

From the material reviewed the following seems to be a reasonable assessment of our present capabilities to predict energy deposition in microelectronic structures:

The material structures for which the greatest uncertainty exists are the thin gate oxides encountered in MOS device structures. Prediction uncertainties are on the order of a factor of two but only part of this can be attributed to the dose calculation. The other important factor in this application is recombination and its dependence on local electric field. The factors that play an important role in the dose uncertainty are as follows:

Uncertainty regarding the cross sections (and the derived quantities such as mean free paths, stopping powers and ranges) for elastic and inelastic interactions of electrons with energies below 10 keV and especially below 1 keV in materials of interest in microelectronics. Note that it has been estimated that 50% of the holes created in gate oxides are produced by electrons with energies below 100 eV. Almost the entire data base in this energy range has emerged from ORNL over the past dozen years with few checks against other measurements or calculations. The uncertainty increases the lower in energy we go and is largest below a few hundred eV.

The cutoff energy in the existing Monte Carlo codes is in the vicinity of 1000 eV which is much higher than the energies of electrons responsible for depositing energies in thin films. Calculations have indicated that below 500 Angstroms a 10 eV cutoff energy may not be low enough. This poses serious problems for Monte Carlo codes in terms of extending the running times.

The condensed history approach used in electron Monte Carlo codes may not be suitable for thin multiple layers of materials. The alternative is to follow each collision which again has the effect of significantly extending the running times.

There are some indications that the cross sections for electrons in the medium energy range may not be adequate from electron backscatter and photon induced electron backscatter.

Input information on the spectrum of the photon source may not be adequate. This has been a persistent problem in commonly used cobalt-60 test sources i.e. gamma cells, concrete rooms or water wells. The number of scattered photons incident on the target device can be as high as 50% and vary markedly in its energy spectrum. The uncertainty can be reduced by employing ion chamber which give a measure of the effective incident energy or the maximum dose enhancement to be expected.

Input information on the device under test i.e. its structure, material composition, and critical dimensions. A few tens of Angstroms can lead to significant differences in calculated dose.

The connection between the dose and the response of the target. Thin gate oxides are a clear example. In that case recombination in the presence of local electric fields can profoundly alter the observed reponse.

SECTION 3
THE DIRECT MEASUREMENT OF DOSE ENHANCEMENT

3.1 BACKGROUND.

The direct calculation of dose enhancement is difficult for two reasons: because of scatter it requires a determination of the gamma photon spectrum at the point of interest (a photon transport problem), followed by a second calculation of the energy deposited by the photon induced secondary electrons in the target structure (an electron transport problem). For the complex three dimensional geometries commonly encountered, Monte Carlo computations are generally required in both cases. Fortunately, improvements in transport codes in recent years have enabled calculations to be made for even the complex multilayered structures typically encountered in device testing. There are additional problems, however, in the routine application of the computational approach.

Accurate input data required to perform the calculations is likely to be unavailable. The photon transport part of the calculation in a given test facility requires data on the exact positions, shapes and compositions of the structures surrounding the test object. The electron transport part of the calculation requires information on the microscopic structural details of the irradiated device or component. Inaccurate information concerning either or both of these areas can render the transport calculations inaccurate.

As indicated in the first part of this report the magnitude of the dose enhancement is very sensitive to the gamma spectrum at the point of interest. This spectrum is very different from that emitted by the source due to Compton scattering within the test facility. The scattered spectrum is also quite variable from one test facility to another. Large variations are even possible in the same facility due to changes in supporting structures or shielding materials in the immediate vicinity of the object under test.

The value of an experimental method for estimating the relative magnitude of the low energy component in any test arrangement of interest was pointed out by Kerris and Gorbics [57]. The experimental information could then be used to obtain an estimate of the dose enhancement factor. The approach described in the present study extends the method employed in [57]. It is based upon earlier work with multicavity chambers [1] and subsequent experience with chambers of that type.

In this section of the report a description of the present approach and its implementation in the form of a dual cavity ionization chamber is given. New results obtained with this chamber are presented to illustrate its capabilities. Possible future applications and modifications are briefly described.

3.2 DESIGN FACTORS.

The approach followed in the present study is based upon the multicavity chambers employed in the first measurements of dose enhancement as shown in Figure 1 [1]. Selection of the basic design was motivated by the desire to achieve the following performance characteristics:

Direct measurements of dose enhancement factors without reference to other experimental or computational data.

A capability to simulate many different conditions encountered in a component under test.

An ability to detect the dependence of the dose on sample orientation.

High spatial resolution so that energy deposition in simulated multilayer structures could be explored.

Ease of use, reliability, accuracy, and simple low cost construction.

The basic design selected for the chamber is shown in Figures 20 and 21. It employs parallel plate geometry with two air cavities 4.5 cm in diameter and walls 0.1 cm apart. The design permits the wall materials to be varied according to the particular problem of interest. In the most typical configuration the electrodes consist of three 0.1 cm thick aluminum plates separated by polystyrene insulators of the same thickness. A 50 μm gold foil is stretched over the interior of the inner electrode in one of the cavities. The thicknesses of the cavity walls used here are based upon previous experimental

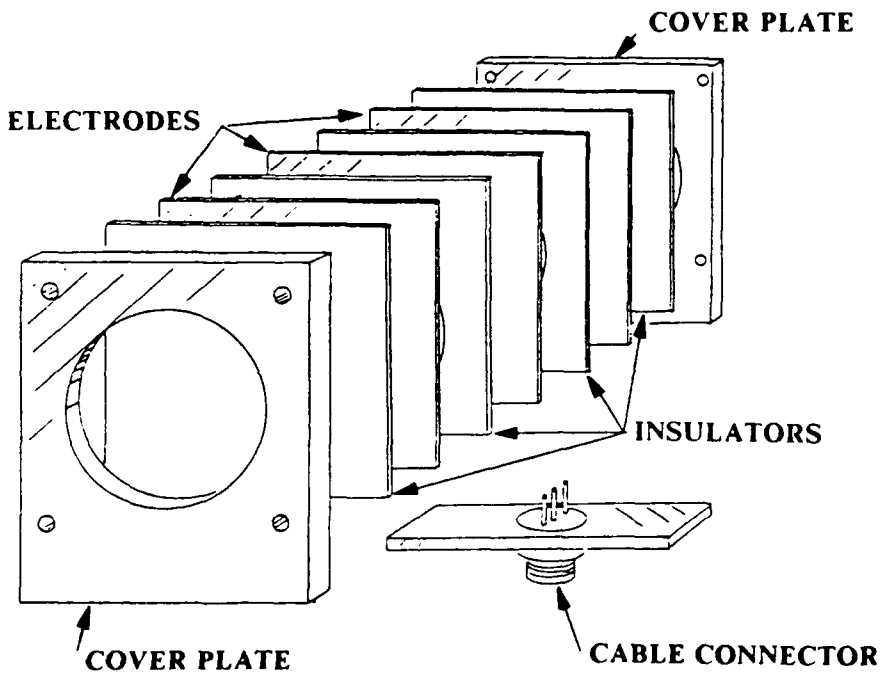

Figure 20. Schematic showing the arrangement of the main components of the dual cavity ionization chamber.

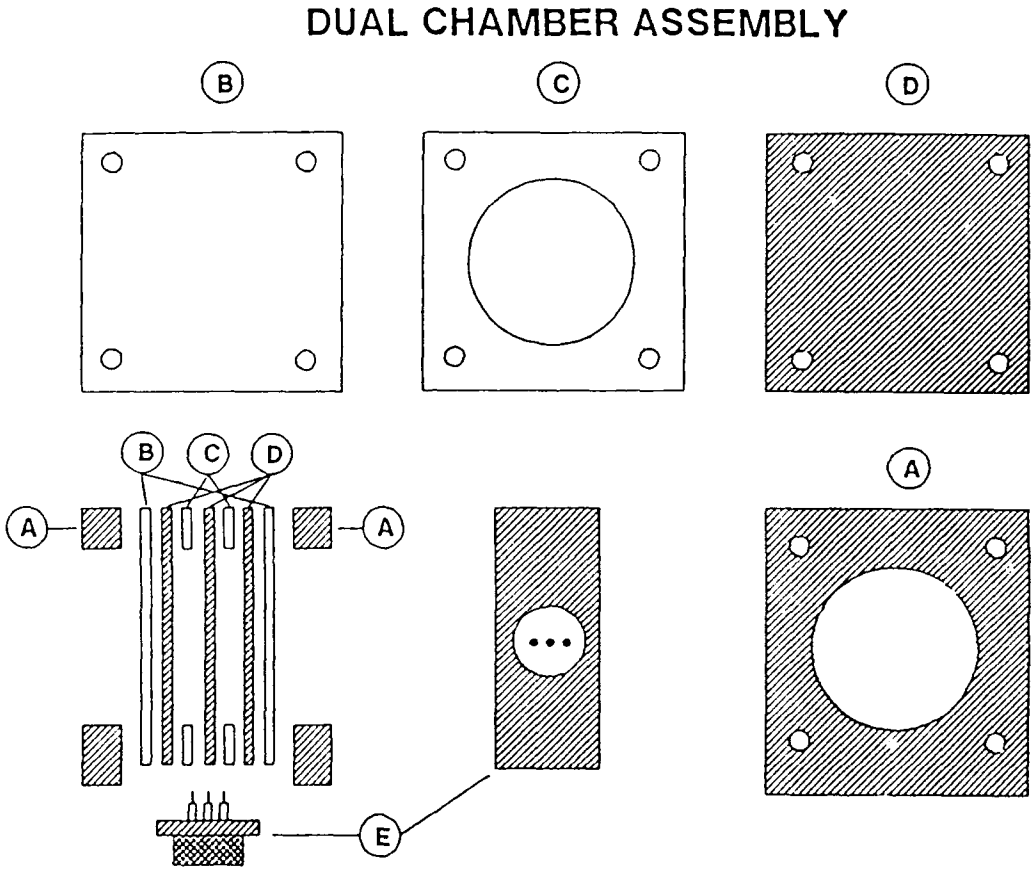

Figure 21. An exploded cross section view of the dual cavity ion chamber with separate end on views of the components. Three electrodes (D) and two polystyrene spacers (C) form the two cavities. Polystyrene end covers (B) are used to reduce external effects. Aluminum end plates (A) clamp the assembly together. A small end plate (E) supports the cable connector.

studies [4]. Solid end covers of polystyrene 0.1 cm thick are used to isolate the electrodes from the external environment and an aluminum frame is employed to clamp the assembly together. The cable conductors are connected to the electrodes by mechanical pressure.

Calculations based upon well established relationships on ion chamber performance [3] show that a chamber of this type should have a collection efficiency of >99% at an exposure rate of 100 R/s. The effect of humidity on response amounts to less than one percent for changes in relative humidity ranging between 5 to 95%.

The basic measuring circuit employed in these studies has been previously described [1] (see Figure 22). It includes a potentiometer and switching circuit for varying the applied potential in either cavity between a few tenths of a volt to $\pm$60 volts.

3.3 PERFORMANCE.

The chambers were found to yield excellent plateau curves for all material and voltage polarity combinations. In obtaining the data reported here readings were taken over a 10 to 60 volt range. The relative standard deviation of the dose enhancement factors obtained over this range typically did not vary by more than 2% which means that applied bias does not need to be rigorously controlled.

A factor that is not often mentioned with regard to the operation of ionization chambers of the type described here is the appearance of polarity effects i.e., changes in the collected current as a function of the polarity of the applied voltage. A number of factors can contribute to this effect [3]. These factors include: contact, thermal, of electrolytic emf's in the measuring circuit. "Compton current" effects, leakage currents picked up from exposed leads and contacts. To eliminate possible errors from this source the readings obtained under positive and negative bias were averaged. If this is not done the enhancement factors may vary by $\pm$5% of those reported here.

The dose enhancement factor for the aluminum immediately adjacent to the gold interface was directly obtained by measuring the ratio between the ionization current in the all aluminum cavity chamber and the mixed aluminum gold foil cavity chamber at the same exposure position. Note that it is not necessary, as in the procedure described by Kerris and Gorbics [57] and outlined in Figure 22 to first obtain an effective energy from an energy response curve followed by an estimate of the enhancement from Monte Carlo calculations of the enhancement factor as a function of energy as shown

in Figure 23. At the present time Monte Carlo calculations of dose enhancement versus photon energy are only available for gold next to silicon and gold next to polyethylene. This restricts the application of the method outlined in [57] to those material combinations. The direct measurement technique does not require data from calculations and can be applied to any combination of materials which are electrically conducting as shown in Figure 24. Also, unlike a single cavity chamber as in [57], only one experimental setup of the dual cavity is required. The two chamber readings needed to arrive at the ratio are obtained directly without changing the chamber configuration or position (see Figures 23 and 24).

3.4 RESULTS.

After ensuring that the observed currents accurately reflected cavity ionization and were not contaminated with induced "Compton currents" or other stray sources the dual chamber was used to explore a series of cases of possible interest. The cobalt-60 Radiation Facility at Hanscom AFB was used in these studies. As a first step the response of the all aluminum chambers were compared with calibrated Victoreen R chambers and found to yield a current within 10% of a calculation based upon the nominal chamber dimensions. It was clear that with calibration it was possible to use the all aluminum cavity of the dual chamber as a "silicon equivalent dosimeter".

The dual chamber was then used in the configuration required for measuring the enhancement at a gold/aluminum interface. In this configuration one of the cavities has a gold foil stretched over the interior aluminum electrode as previously described. In earlier work it had been found that surrounding a chamber with paraffin would increase the Compton scatter sufficiently to markedly increase the dose enhancement factor [37]. When lead was substituted for the paraffin the enhancement factor was noticeably reduced. In the experiments with the dual chamber exposures were made with paraffin (10 cm), lead (0.2 cm) and the normal exposure conditions (no material between the source and chamber other than air). The results are shown in the upper part of Table 4.

The wax was 10 cm thick and lead 0.2 cm. The relative standard deviation (r/l) for the dose enhancement factors (DEF's) did not vary by more than 2%.

The scatter medium is shown in the first column (e.g. Air for normal exposure), the orientation of the wall materials in the second column (e.g. Al ≥ Au means that the cobalt-60 photons penetrate the aluminum before reaching the interface with the gold), and the last column gives the observed enhancement factor.

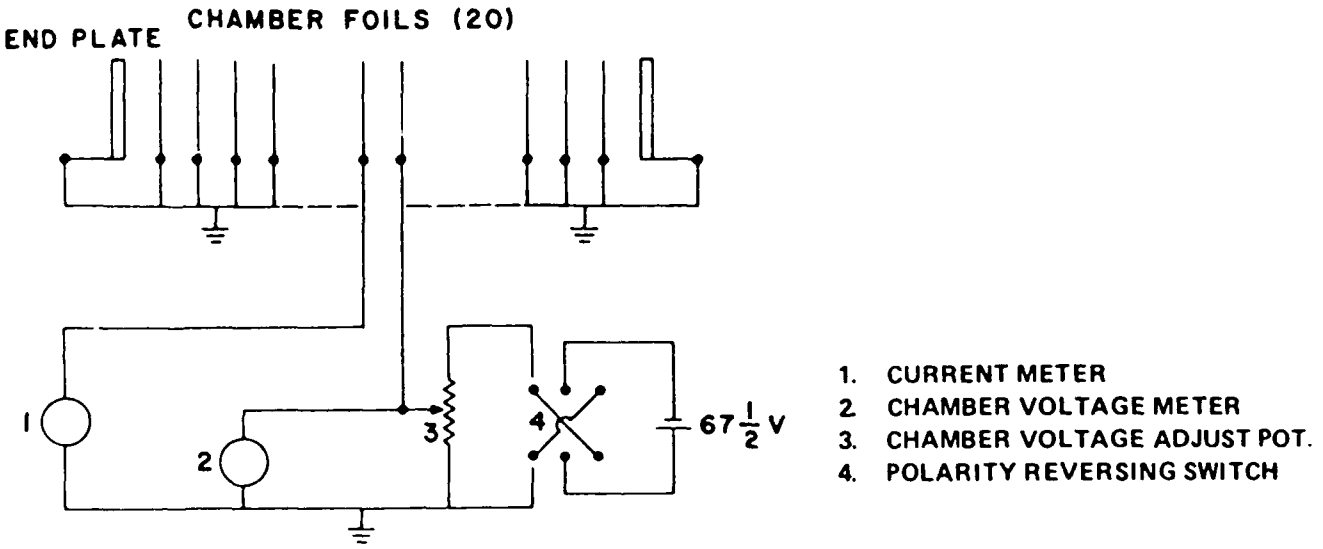

Figure 22. Schematic of chamber current measuring circuit.

MEASUREMENT PROCEDURES COMPARED

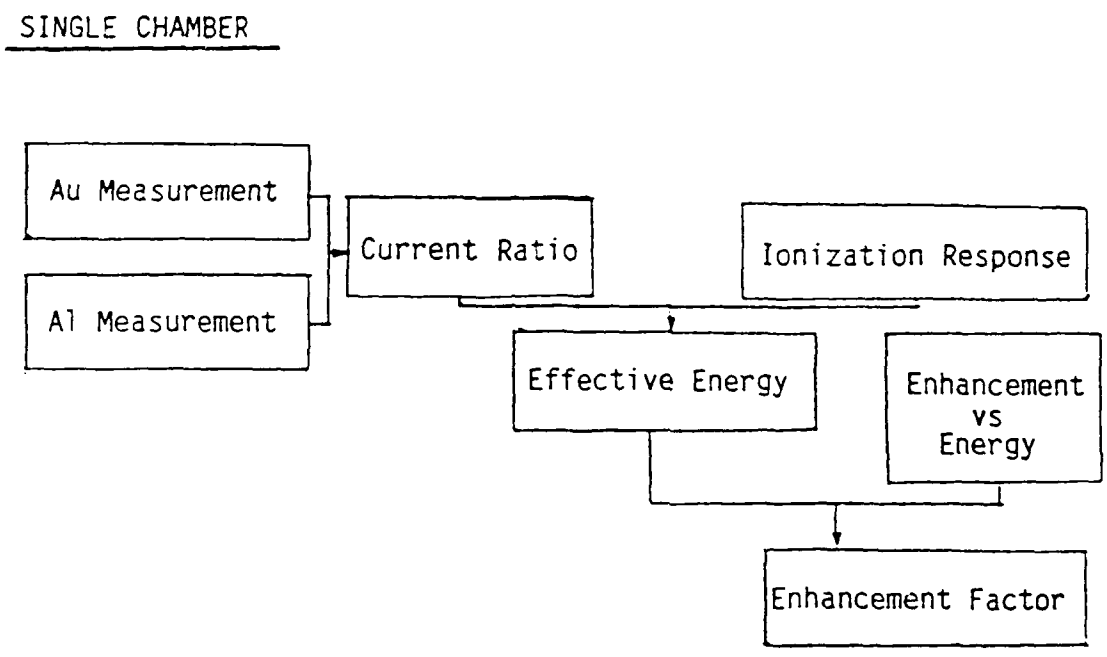

Figure 23. Procedure for deriving an enhancement factor from separate gold and aluminum ion chambers [57].

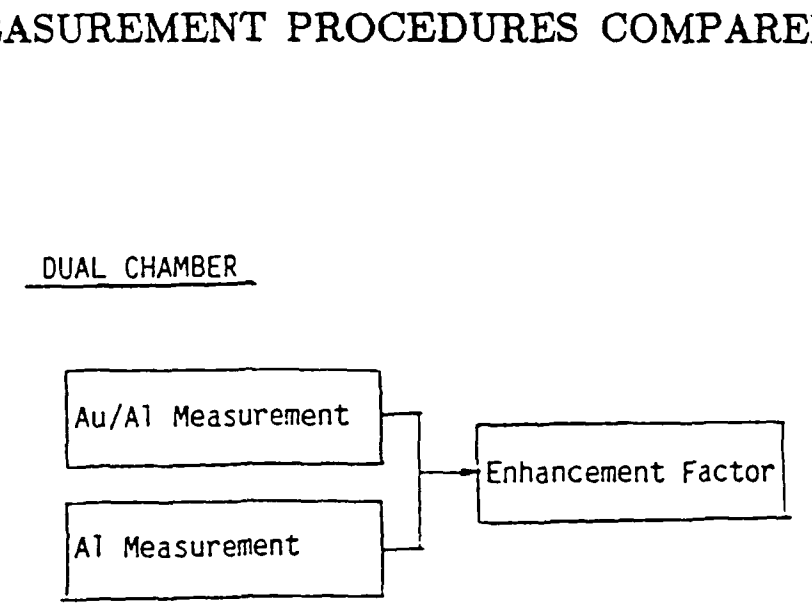

Figure 24. Procedure for deriving an enhancement factor from the dual ionization chamber.

Table 4. Experimental dose enhancement factors (DEF).

Scatter Medium	Chamber Configuration	DEF
Air	Al ≥ Au	2.03
Air	Au ≥ Al	1.51
Wax	Al ≥ Au	2.39
Wax	Au ≥ Al	1.89
Lead	Au ≥ Au	1.56
Lead	Au ≥ Al	1.03
Air	Cu ≥ Au	1.72
Air	Au ≥ Cu	1.46
Wax	Cu ≥ Au	1.91
Wax	Au ≥ Cu	1.59
Lead	Cu ≥ Au	1.36
Lead	Au ≥ Cu	1.13

Note: The orientation of the wall materials is indicated in the second column. For example Al ≥ Au means that cobalt-60 photons penetrate the aluminum chamber wall prior to interacting with the gold. The wax was 4" thick and the Pb 0.084".

The dose enhancement factor for the Al ≥ Au orientation was found to be 2.03. This is a typical value for the case where the photons approach the interface from the low atomic number side. Note that when the beam direction is reversed the dose enhancement factor is reduced by about 25%. This demonstrates the importance of the orientation effect which has frequently been ignored in piece part testing. The magnitude of the orientation effect varies with scatter conditions and distance from the interface. It is readily detected with a dual chamber of the type described here.

The orientation effect will be most important when the primary photons impinge upon the target from one direction. In the case of cylindrically symmetric sources e.g. gammacells, or in certain configurations encountered in water pools, the primary photons and the associated Compton scattered photons penetrate the interface from opposing directions. This tends to reduce, and in the case of perfect symmetry remove, the dependence on orientation. The dose enhancement, however, remains yielding a value representing an average over the two extremes found in a directional source.

The influence of enhancing the Compton scatter is evident in the next pair of readings where the scatter medium is 10 cm of paraffin wax. The enhancement factors are observed to increase markedly for both beam directions. The assumption that the "high energy" cobalt-60 photons should be little influenced by this relatively small amount of low atomic number material is misleading. In a real test situation the material might be plastic, wood or water.

Finally we see the result of adding a high atomic number filter to reduce the amount of Compton scatter. The enhancement factors are reduced but the asymmetry remains. Note that with these particular combinations of scatter materials the difference between the lowest and highest dose enhancement factor is a factor of two.

An alternative way of comparing variations in dose enhancement is to compare changes in the enhanced dose only i.e. subtract 1.0 from the usual dose enhancement factor. A change in a DEF from 2.0 to 1.5 then represents a 50% rather than a 25% change in enhancement. However, in the present paper we will use the more common method of comparing dose enhancement factors.

It is significant that all of these readings were taken in exactly the same position in the RADC concrete shielded exposure facility. Only relatively small changes were made in the scatter environment by adding wax bricks or small amounts of lead shielding. Such materials can frequently find their way into test facilities of this sort without attracting much concern. Much larger changes can occur if the target is moved next to large sources of scatter such as the shielding walls. This potential for inadvertently changing the exposure conditions is an important reason for employing a chamber of the type described here.

In addition to studies with the Au/Al chamber a series of runs were carried out with an all copper chamber (rather than aluminum) one cavity of which contained a gold foil. In this case we can consider the combination as closely simulating the ionization dose enhancement conditions at a gold - gallium arsenide interface. It was found in early experimental studies [1] that materials with intermediate atomic number gave very similar profiles.

As can be seen from Table 4 the enhancement factors are only slightly lower than the Au/Al case. The Compton scatter, enhanced by the paraffin, strongly influences the result. These are the first reported measurements for a case corresponding to what might be observed in a gallium arsenide device. In this case the experimental results when a lead filter is present are in excellent agreement

with past calculations [58]. The calculations were done for pure cobalt-60 photons and the lead filter brings the incident spectrum close to that condition. The calculated values were 1.35 and 1.16 and the measured values are 1.36 and 1.13.

It is essential that the enhancement factors in the ionizing dose reported here not be automatically applied to the introduction of displacement damage in gallium arsenide devices. It turns out that displacement damage enhancement can also occur at gamma irradiated interfaces as described in some detail by Garth et al [58]. The problem is that the amount of damage is very sensitive to the threshold energy for displacement as pointed out by Meulenberg et al [59]. A change in the threshold from 10 eV to 25 eV means that the lowest energy electrons effective in producing damage changes from 250 keV to 600 keV This means that the Compton scatter effect, which can markedly enhance the ionization dose by increasing the low energy electron fluence at the interface, is likely to have little if any effect on displacement damage. References [58] and [59] should be consulted for further information on this problem.

One of the interesting capabilities of the dual chamber described is that it can be used to determine the enhancement at any distance from the interface by simply adding an intervening foil. This was done for aluminum and yielded results corresponding to those given in Figure 1. Any complex multilayer structure can be thus be simulated provided that the outer layers are conducting.

To obtain a dose profile additional cavities could be added up to the twenty employed in the original studies, however, ease of use declines proportionally. An attractive alternative is to combine the experimental readings obtained by adding additional foils with calculations using a code such as that developed by Garth [58]. Since the cobalt-60 generated spectra tend to fall within narrow bounds the experimental determinations should be sufficient to enable a useful dose profile to be generated.

Finally some comments should be included relative to the quantitative correlation between dose enhancement factors as determined with the dual cavity chamber, and measurements of dose enhancement using devices [32]. The primary advantage of the dual chamber is that it can be used to readily detect any inadvertent changes in the irradiation environment that might significantly alter the dose enhancement factor in vulnerable devices. Note that the dual cavity chamber measures the maximum dose enhancement factor in aluminum immediately next to gold. The sensitive regions of most devices exposed to the same environment would normally be some distance from the interface. Consequently, the chamber can be considered to establish an upper bound to the dose enhancement effect. It also affords the possibility of closely simulating many types of configurations in IC circuit

packages and independently determining the dose enhancement. It thereby affords a check on computer code calculations. However, in many cases, as previously discussed, it has been found that the response of devices cannot be simply correlated with dose enhancement e.g see [55] Nevertheless it is useful to have an independent measure of the actual dose as differentiated from the response. It is worth mentioning that the magnitude of the dose enhancement effect, the influence of orientation relative to directed sources, and the importance of Compton scatter were all first detected with ionization chambers.

3.5 SUMMARY OF RESULTS.

A dual cavity ionization chamber has been designed, fabricated, tested and applied to measure dose enhancement factors under a wide range of conditions. It proved to be an efficient method for determining the enhancement factors for the highly variable conditions encountered in actual testing. The chamber can be calibrated to give an absolute dose reading for silicon, gallium arsenide, or any other material together with the associated enhancement factor. It also can be used as a research tool to measure enhancement factors for material combinations not previously examined. Dose response curves or parametric Monte Carlo calculations (both of which can be difficult to obtain) are not required to apply the method.

SECTION 4
CONCLUSIONS

A survey of all relevant literature concerning dose enhancement was carried out and a selective review of that information is presented in this report. Much of hoe information covered has received only limited distribution in the past. Looking beyond the immediate problem of predicting and correlating the response of MOS devices to cobalt-60 and 10 keV X-rays the fundamental issue is how accurately the absorbed dose in the vicinity of boundaries can be predicted. N particular is the basic physics understood.

The available evidence reviewed here indicates that only for MOS device response have problems arisen. In that case the dose enhancement acts together with recombination and local electric fields to modify the observed response. It would, at first glance, appear reasonable to attribute the factor of two uncertainty encountered in these cases all to the recombination process. However, in 1986 evidence was presented which showed that calculations of the dose in thin oxide layers was very sensitive to the energy cutoff point. Most Monte Carlo codes cutoff at energies around 1 keV while the new results suggested that 10 eV might not be sufficient. It was also shown that more than half of the holes in an oxide are generated by electrons with energies less than 100 eV. To date this issue has not been resolved.

It does not appear that a direct experimental test of existing theory to calculate energy deposition down to low energies could be made independent of the complications that occur in oxides. This could be done using the mechanisms of low energy secondary emission. In that case we have extensive experimental and theoretical evidence accumulated over decades to refer to. it can test our capabilities to predict energy deposition and electron transport down to an electron volt or less. Recombination and other complications associated with oxides are not involved.

SECTION 5
LIST OF REFERENCES

1. J. A. Wall and E. A. Burke, "Gamma Dose Distributions At and Near the Interface of Different Materials", IEEE Trans. Nucl. Sci., NS-17, 305-309 (Dec.1971).

2. A. R. Frederickson and E. A. Burke, "Ionization, Secondary Emission, and Compton Currents at Gamma-Irradiated Interfaces", IEEE Trans. Nucl. Sci., NS-18, 162-169 (Dec.1971).

3. F. H. Attix, Introduction to Radiological Physics and Radiation Dosimetry, John Wiley & Sons, New York (1986).

4. W. H. Bragg, "Consequences of the Corpuscular Hypothesis of the Gamma and X-rays, and the ranges of Beta Rays", Phil. Mag., 20, 385 (1910).

5. L. H. Gray, "Absorption of Penetrating Radiation", Proc. Roy. Soc. (London), A122, 647 (1929)

6. F. H. Attix, Introduction to Radiological Physics and Radiation Dosimetry, John Wiley & Sons, New York (1986).

7. T. E. Burlin, J. M. Sidwell, and B. M. Wheatley,"Application of Monte Carlo Methods in Medical Radiology", Brit. J. Radiology, 46, 398-399 (1973).

8. E. Kearsley,"A New General Cavity Theory", Phys. Med. Biol., 29, 1179-1187 (1984).

9. E. A. Burke and J. C. Garth,"An Algorithm for Energy Deposition at Interfaces", IEEE Trans. Nucl Sci., NS-23(6), 1838-1843 (1976).

10. W. L. Chadsey," X-Ray Dose Enhancement", IEEE Trans. Nucl. Sci., NS-25 (6), 1591-1597 (1978).

11. J. C. Garth, "An Algorithm for Calculating Dose Profiles in Multilayered Devices Using a Personal Computer", IEEE Trans. Nucl. Sci., NS-33, 1266-1272 (Dec.1983).

12. F. W. Spiers," Transition-Zone Dosimetry", in Radiation Dosimetry, 2nd ed., Vol.3, F. H. Attix and E. Tochilin, Eds., Academic Press, New York, 809-867 (1969).

13. J. Dutreix and M. Bernard," Dosimetry at Interfaces for High Energy X and Gamma Rays", Brit. J. Radiol. 39, 205-210 (1966).

14. K. W. Dolan and J. L. Wirth," Non-Local Energy Deposition in Silicon by Energetic Photons", IEEE Annual Nuclear and Space Radiation Effects Conference, Summaries of Papers, 215-217 (July 1969).

15. L. S. Mims and R. A. Williams," Effects of Packaging on Radiation-Induced Responses", IEEE Annual Nuclear and Space Radiation Effects Conference, Summaries of Papers, 219-222 (July 1969).

16. E.A. Burke, J.R. Cappelli, L.F. Lowe, and J.A. Wall, "Solar Cell Radiation Response Near the Interface of Different Atomic Number Materials", AFCRL-72-0045, 15 (24 November 1971).

17. E.A. Burke, A.R. Frederickson, J.C. Garth and J.A. Wall, "Secondary Electron Phenomenology", Annual Technical Report, DNA Subtask TA040, 21 (May 1971).

18. C. H. Sherman and N. E. Gordan, "Calculation of the Radiation Dose at the Interface Between Dissimilar Media", Parke Mathematical Laboratories Tech. Memo. No. 16, (August 1970).

19. D. E. Charlton and D. V. Cormack, Radiation Research, 17,34-49 (1962).

20. J. A. Wall and E. A. Burke," Dose Distributions At and Near the Interface of Different Materials Exposed to Cobalt-60 Gamma Radiation", AFCRL-TR-75-0004, 29 (17 December 1974).

21. M. J. Berger,"Absorbed Dose Near an Interface Between Two Media", NBS Report 10 550, 38-48 (March 1971).

22. W. L. Chadsey," Monte Carlo Analysis of X-Ray and Gamma Ray Transition Zone Dose and Photo-Compton Current", AFCRL-TR-73-0572, 50 (November 1973).

23. E. A. Burke, J. R. Cappelli, L. F. Lowe and J. A. Wall," Solar Cell Radiation Response Near the Interface of Different Atomic Number Materials", AFCRL-72-0045,15 (24 November 1971).

24. T. A. Dellin, K. W. Dolan and C. J. MacCallum," Photo-Compton Currents at Material Interfaces: Theory and Experiment", IEEE Trans. Nucl. Sci., NS-21(6), 227-234 (1974).

25. S. Woolf and E. A. Burke, "Monte Carlo Calculations of Irradiation Test Photon Spectra", IEEE Trans. Nucl. Sci., NS-31, 1089-1094 (Dec. 1983).

26. L. F. Lowe, W. C. Taylor and J. R. Cappelli," Interface Dose as a Function of Angle of Incidence for Aluminum-Gold and Aluminum-Beryllium Slabs", AFCRL-TR-75-0206, 9 (11 April 1975).

27. W. L. Chadsey," POEM: A Fast Monte Carlo Code for the Calculation of X-Ray Photoemission and Transition Zone Dose and Current," AFCRL-TR-75-0324,105 (January 1975).

28. D. M. Long and D. H. Swant," Dose Gradient Effects on Semi-conductors", AFCRL-TR-74-0283, 99 (July 1974).

29. R.A. Berger and J.L. Azarewicz," Packaging Effects on Transistor Radiation Response," IEEE Trans. Nucl. Sci., NS-22(6), 2568-2572 (December, 1975).

30. D.M. Long, D.G. Millward and J. Wallace," Dose Enhancement Effects in Semiconductor Devices", IEEE Trans. Nucl. Sci., NS-29(6), 1980-1984 (December, 1982).

31. D. M. Long, D. G. Millward, R. L. Fitzwilson, and W. L. Chadsey, "Handbook for Dose Enhancement Effects in Electronic Devices", RADC-TR-83-84 (March 1983).

32. M. J. Berger, "Monte Carlo Calculation of the Penetration and Diffusion of Fast Charged Particles", in Methods in Computational Physics Vol 6, edited by B. Alder, S. Fernbach, and M. Rotenberg, Academic Press, New York (1960) Chapt. V.

33. W. L. Chadsey, J. C. Garth, R. L. Sheppard, and R. Murphy," X-Ray Dose Enhancement Vol.I: Summary Report", RADC-TR-76-159, 89 (May 1976).

34. T. A. Dellin and C. J. MacCallum," Analytical Photo-Compton Deposition Profiles", IEEE Trans. Nucl. Sci., NS-23(6), 1844-1849 (1976).

35. E. A. Burke and J. C. Garth,"Energy Deposition by Soft X-Rays - An Application to Lithography for VLSI", IEEE Trans. Nucl. Sci., NS-26(6), 4868-4873 (1979).

36. D.B. Brown," Photoelectron Effects on the Dose Deposited in MOS Devices by Low Energy X-Ray Sources", IEEE Trans. Nucl. Sci., NS-27(6), 1465-1468 (December 1980).

37. L.F. Lowe, J.R. Cappelli and E.A. Burke," Dosimetry Errors in Co-60 Gamma Cells Due to Transition Zone Phenomena", IEEE Trans. Nucl. Sci., NS-29(6), 1992-1995 (December 1982).

38. D.B. Brown and C.M. Dozier,"Reducing Errors in Dosimetry Caused by Low Energy Components of Co-60 and Flash X-Ray Sources", IEEE Trans. Nucl. Sci., NS-29(6), 1996-1999 (December 1982).

39. ASTM Committee E-10,"Minimizing Dosimetry Errors in Radiation Hardness Testing of Silicon Electronic Devices Using Co-60 Sources," Standard E 1249-88, 1988 Annual Book of ASTM Standards, Vol.12.02, ASTM, Philadelphia, 762-777 (September 1988).

40. S. Woolf and A.R. Frederickson," Photon Spectra in Cobalt-60 Gamma Test Cells," IEEE Trans. Nucl. Sci., NS-30(6), 4371-4376 (December 1983).

41. S. Woolf and E.A. Burke,"Monte Carlo Calculations of Irradiation Test Photon Spectra", IEEE Trans. Nucl. Sci., NS-31(6), 1089-1094 (1984).

42. J.G. Kelly, T.F. Luera, L.D. Posey, D.W. Vehar, D.B. Brown and C.M. Dozier,"Dose Enhancement Effects in MOSFET IC's Exposed in Typical Co-60 Facilities", IEEE Trans. Nucl. Sci., NS-30(6), 4388-4393 (December 1983).

43. L. J. Palkuti," Comprehensive Radiation Testing of ICs at the Wafer Stage," Presented at the IEEE 1984 Annual Conference on Nuclear and Space Radiation Effects, 16 (July 1984).

44. T. R. Oldham and J. M. McGarrity, "Comparison of Cobalt-60 Response and 10 keV X-Ray Response in MOS Capacitors", IEEE Trans. Nucl. Sci., NS-30(6), 4377-4381 (December 1983).

45. C. M. Dozier and D. B. Brown, "The Use of Low Energy X-Rays for Device Testing - A Comparison with Co-60 Radiation", IEEE Trans. Nucl. Sci., NS-30, 4382-4387 (December 1983).

46. D. M. Fleetwood, P. S. Winokur, R. W. Beegle, P. V. Dressendorfer, and B. L. Draper,"Accounting for Dose Enhancement Effects With CMOS Transistors", IEEE Trans. Nucl. Sci., NS-32, 4369-4375 (Deccember 1985).

47. C. M. Dozier, D. M. Brown, J. L. Throckmorton and D. I. Ma, "Defect Production in SiO_2 by X-ray and Co-60 Radiations", IEEE Trans. Nucl. Sci., NS-32, 4363-4375 (December 1985).

48. C. M. Dozier, D. M. Brown, R. K. Freitag, and J. L. Throckmorton "Use of the Subthreshold Behavior to Compare X-ray and Co-60 Radiation Induced Defects in MOS Transistors", IEEE Trans. Nucl. Sci., NS-33, 1324-1329 (December 1986).

49. J. M. Benedetto and H, Boesch, The Relationship Between 60Co and X-Ray Damage in MOS Devices", IEEE Trans. Nucl. Sci , NS-33, 1318-1323 (December 1986).

50. D. M. Fleetwood, P.S. Winokur, L.J. Lorence Jr.,W. Beezhold, P. V. Dressendorfer and J.R. Schwank,"The Response of MOS Devices to Dose-Enhanced Low Energy-Radiation," IEEE Trans. Nucl. Sci., NS-33(6), 1245-1251 (1986).

51. R.N. Hamm,"Dose Calculations for Si-SiO2Si Layered Structures Irradiated by X Rays and 60Co Gamma Rays," IEEE Trans. Nucl. Sci.,NS-33(6),1236-1239 (1986).

52. D.B. Brown," The Phenomenon of Electron Rollout for Energy Deposition and Defect Generation in Irradiated MOS Devices," IEEE Trans. Nucl. Sci., NS-33(6), 1240-1244 (1986).

53. D. E. Beutler, D. M. Fleetwood, W. Beezhold, D. Knott, L. J. Lorence, Jr., and B. L. Draper, "Variations in Semiconductor Device Response in a Medium Energy X-Ray Dose Enhancing Environment", IEEE Trans. Nucl. Sci., NS-34, 1544-1550 (Dec.1987).

54. D. M. Fleetwood, D. E. Beutler, L. J. Lorence Jr., D. B. Brown, B. L. Draper, L. C. Riewe, H. B. Rosenstock, and D. P. Knott, "Comparison of Enhanced Device Response and Predicted X-Ray Dose Enhancement Effects on MOS Oxides", IEEE Trans. Nucl. Sci., NS-35, 1265-1271 (December 1988).

55. J. M. Benedetto and H, Boesch, "Dose and Energy Dependence of Interface Trap Formation in Cobalt-60 and X-Ray Environments", IEEE Trans. Nucl. Sci., NS-35, 1260-1264 (Dec.1988).

56. C.J. Tung and C.P. Wang,"Multiple Scattering of Low Energy Electrons in Aluminum," IEEE Trans. Nucl. Sci., NS-30(6), 4409-4412 (December 1983).

57. K. G. Kerris and S. G. Gorbics, "Experimental Determination of the Low Energy Component of Cobalt-60 Sources", IEEE Trans. Nucl. Sci., NS-32, 4356-4362 (December 1985).

58. J. C. Garth, E. A. Burke and S. Woolf, "Displacement Damage and Dose Enhancement in Gallium Arsenide and Silicon", IEEE Trans. Nucl. Sci., NS-32, 4382-4387 (December 1985).

59. A. Meulenberg, C. M. Dozier, W. T. Anderson, S. D. Mittleman, M. H. Zugich, and C. E. Caefer, "Dosimetry and Total Dose Radiation Testing of GaAs devices", IEEE Trans. Nucl. Sci., NS-34, 1745-1750 (December 1987).

60. A.M. Kellerer, "Fundamentals of Microdosimetry", in The Dosimetry of Ionizing Radiation Vol. 1, K.R. Kase et al, Eds. Academic Press, New York (1985).

61. E.A. Burke, "Ionizing Events in Small Device Structures", IEEE Trans. Nucl. Sci., NS-35, 1203-1207 (1988).

62. R.K. Freitag, E.A. Burke, C.M. Dozier and D.B. Brown, "The Development of Non-Uniform Deposition of Holes in Gate Oxides", IEEE Trans. Nucl. Sci., NS-35, 1203-1207 (1988).

63. R. K. Freitag, E. A. Burke, C. M. Dozier, and D. B. Brown,"The Development of Non-Uniform Deposition of Holes in Gate Oxides", IEEE Trans. Nucl. Sci., NS-35, 1203-1207 (1988).

APPENDIX A
DOSE FLUCTUATIONS

A.1 BACKGROUND.

As mentioned in the summary of the literature review of dose enhancement the first step in correlating the effects of different types of radiations or the effects of different energies of the same radiation is to determine by calculation or measurement the energy imparted to the sensitive regions of the target. As microelectronic devices have evolved their dimensions have dropped so that basic assumptions upon which standard theoretical and experimental dosimetry is based can lead to serious errors. One of the problems that has arisen as a result of reduced device dimensions is dose enhancement which is the main topic addressed in this report. Anotner problem that has not received much notice to date is that of fluctuations in the dose delivered to a small target. This problem first arose in connection with optical sensors containing large numbers of sensitive pixels. It was found in those cases that significant statistical variations in device response occurred for both ionizing effects and displacement damage. It was also found that it was possible to quantitatively describe those effects with a general probalistic model [60,61].

Most recently evidence has arisen which indicates that statistical variations may be the cause of so called lateral non-uniformities (LNU's) in the production of holes in gate oxides by X-rays or gamma rays. This raises the question as to how different 10 keV X-rays and cobalt-60 gamma rays are in producing dose fluctuations. That is the topic introduced in this Appendix.

The approach outlined in the following treatment uses established methods originally developed in microdosimetry theory. All of the factors that contribute to fluctuations in the dose are considered. These include the number of Compton and photoelectron hits, the energy spectrum of these electrons, their path length through the gate oxide, and energy straggling by the incident electrons.

The results indicate that the X-ray dose exhibits somewhat larger fluctuations than is the case for gamma radiation over the range of sizes studied. The contribution of the variation in the number of electron interactions to the total variance (the Poisson component), is found to differ for 10 keV X-rays compared to cobalt-60 gamma rays. This component diminishes as the size is reduced.

In the following Appendix the method employed to make the calculations is first described and example calculations given. The results are then compared to recent experimental measurements. Finally, the theory is used to illustrate the variation in dose as a function of device dimensions.

A.2 THEORY OF DOSE FLUCTUATIONS.

The variation of energy deposited in a small target is affected by four kinds of fluctuations:

1) The number of electron tracks that traverse the microvolume is a statistical quantity. It is governed by P' isson statistics.

2) The energy spectrum of the electrons entering the target covers a wide range leading to variations in the rate of energy loss per unit electron track (linear energy transfer). The applicable statistics are derived from transport analysis.

3) The length of the track through the microvolume is a source of fluctuations. It is a sensitive function of the geometric shape and is analyzed using concepts derived from geometrical probability theory.

4) For a given incident electron energy and track length there are still variations in the energy transferred to the target due to energy straggling.

All of the above factors must be taken into account in order to arrive at an estimate of the dose fluctuations in an X-ray or gamma environment.

The models appropriate for handling fluctuations of this type was originally developed we take as a measure of the fluctuations the dimensionless quantity s_D/m_D where s_D is the standard deviation of the absorbed dose and m_D is the average dose. The quantity s_D/m_D can be calculated from microdosimetry theory from the ratio of the first and second moments of the four factors itemized above. The key equations are

$$s_D/m_D = (Z/m_D)^{1/2} \qquad \text{(A.1)}$$

where

$$z = (1.6x10^{-11}/V\ \rho)\ [(\delta^2/\delta) + (L^2/L)(s^2/s)] \qquad \text{(A.2)}$$

where δ^2/δ are the moments of the straggling distribution in keV, L^2/L the moments of the LET distribution in keV/lm and s^2/s the track length moments in lm. V is the volume in cm^3, and ρ the density in g/cm^3. A derivation of these results has been given in the literature [61].

A.3 APPLICATIONS OF FLUCTUATION THEORY.

The results of applying this theory are given in Table 5. The calculations were done for right circular cylinders of SiO_2 with thicknesses of 25, 50, and 100 nm with radii given by r/T_{ox} = 8.5 where Tox is the thickness of the oxide layer. The results presented are for both 10 keV X-rays and cobalt-60 gamma radiation for a nominal exposure of 100 krad. The columns in the Table labelled $N^{-1/2}$ are the contribution to s_D/m_D from the Poisson contribution alone. This is always smaller than s_D/m_D.

Table 5. Relative standard deviation for 100 krad and r/T_{ox} = 8.5.

OXIDE THICKNESS (nm)	GAMA CASE		X-RAY CASE	
	s_D/m_D	$N^{-1/2}$	s_D/m_D	$N^{-1/2}$
100	0.017	0.0052	0.030	0.019
50	0.043	0.010	0.066	0.038
25	0.11	0.021	0.14	0.076

Note that the relative variation is markedly increased for the thin oxides compared to thick layers. Also the relative importance of the Poisson contribution varies for the two radiations. The Poisson factor accounts for about one half the X-ray variation but only about one fifth of that due to cobalt-60.

Results of the theory outlined here have been compared with experiment and found to agree very well with the data. Reference [62] should be consulted for details.

In view of the reasonable agreement between theory and experiment projections have been made of the spread in absorbed dose as a function of oxide thickness. The results are shown in Figure 25. For a total dose of 100 krad it can be seen that for 100 Angstrom films the average dose loses much of its quantitative meaning. There is a finite probability that the dose of a particular film might range anywhere between 5 to 200 krads. The problem of correlating different types of radiations with small experimental samples is clear.

In addition, large gate arrays will guarantee that the extremes of the distribution will occur. The result is shown in Figure 26 where for a sample of 10,000 gates with a thickness of 250 Angstroms the distribution of the extreme dose values is given. It can be seen that it is certain that the largest dose will exceed 145 krads for a mean dose of 100 krads.

A.4 SUMMARY OF FLUCTUATION THEORY.

The preceding short review has shown that dose fluctuations are a problem when devices reach dimensions typical of those now in production. The statistical spread in small samples used in radiation testing will make it difficult to correlate the effects of different radiation types. Theory indicates that there is a real difference between 10 keV X-rays and cobalt-60 gamma rays but this could be very difficult to see experimentally. It also turns out that the maximum deviations are expected to occur for 100 keV X-rays. Experimental information to confirm that prediction is not yet available.

It does appear that a direct experimental test of existing theory to calculate energy deposition down to low energies could be made independent of the complications that occur in oxides. This could be done using the mechanism of low energy secondary emission. In that case we have extensive experimental and theoretical evidence accumulated over decades to refer to. It can test our capabilities to predict energy deposition and electron transport down to an electron volt or less. Recombination and other complications associated with oxides are not involved.

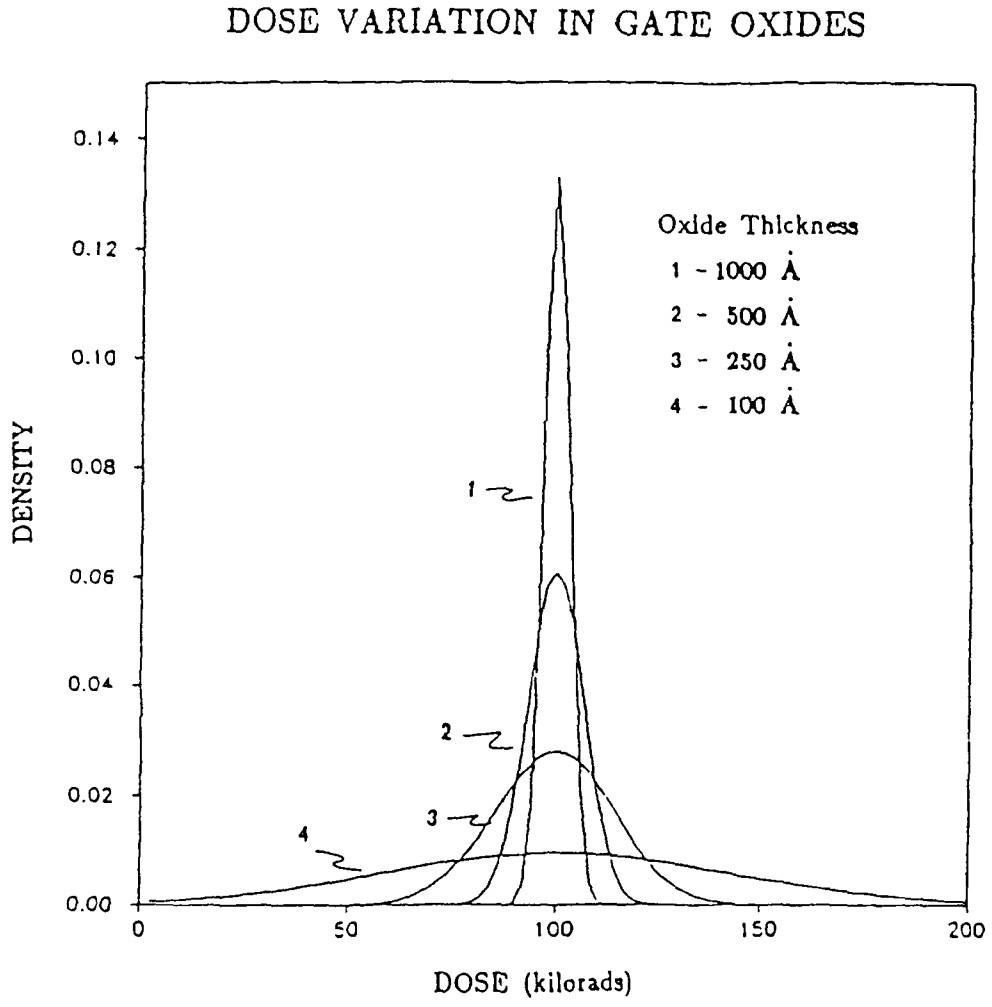

Figure 25. Distribution of absorbed dose in oxides of different thicknesses for 10 keV X-rays.

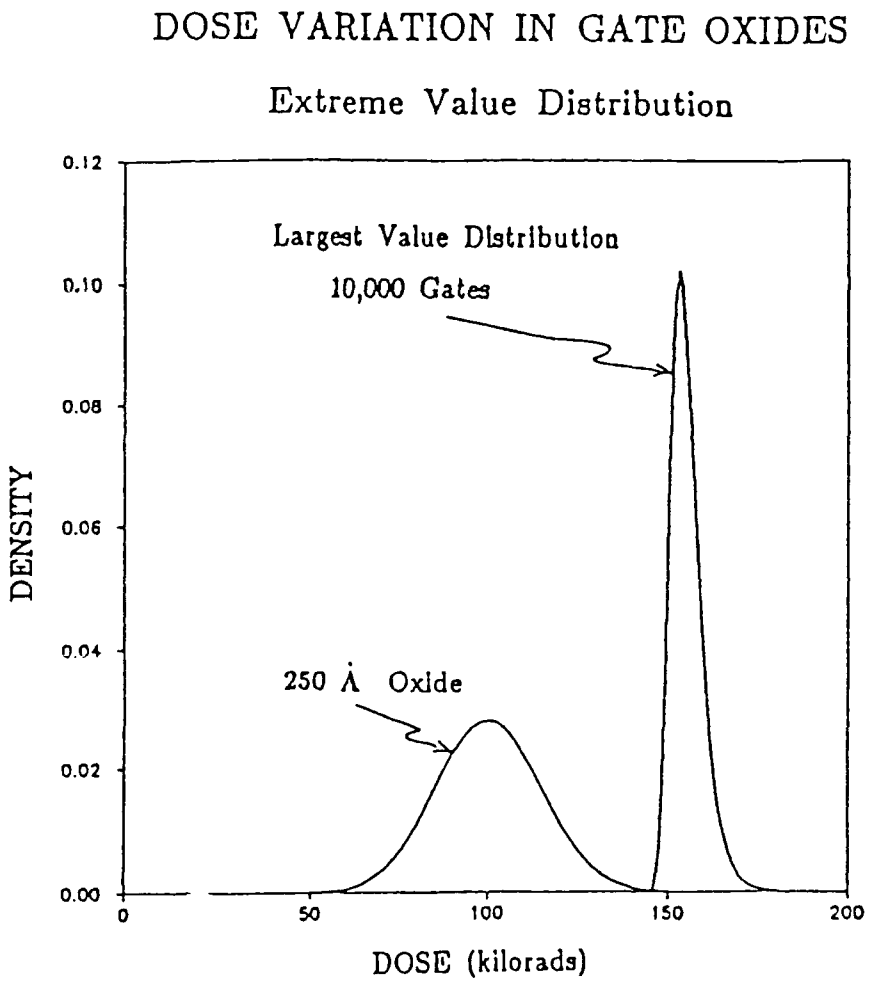

Figure 26. The distribution of the largest dose received by an oxide gate in a sample of 10,000 gates.

APPENDIX B
MEASUREMENT OF X-RAY DOSE ENHANCEMENT

B.1 BACKGROUND.

Studies of MOS device response precipitated questions concerning the accuracy of the computer codes used to calculate dose enhancement into the X-ray region. In the case of these devices it is very difficult to isolate the dose enhancement effect from the recombination mechanism and the latter's sensitivity to local electric fields. It would be highly desirable to check does enhancement calculations using a mechanisms that is free of recombination or other complicating factors.

There are at least three methods which could be employed for making such measurements. These include secondary electron emission detectors, extrapolation ionization chambers, and solid state detectors. Of these, the secondary emission chamber offers the best opportunity to produce a result analogous to what is obtained with the ionization changer at gamma ray energies. It should prove reliable, relatively easy to interpret, and simple to construct. The factors considered in arriving at this conclusion are outlined in the next section.

B.2 FACTORS CONSIDERED IN X-RAY DETECTOR DESIGN.

B.2.1 Features Desired.

Sensitivity - An emission chamber must yield enough current at the anticipated exposure level to provide a reasonable signal to noise ratio.

Spatial Resolution - This is the most difficult goal to satisfy at 10 keV X-ray energies. The target of ultimate concern may consist of a silicon dioxide layer no more than a few Angstroms thick. If the phenomenon employed to observe the dose enhancement integrates over a thickness much larger than that, it will not yield a dose enhancement measurement that is sufficiently accurate. The thickness of material from which secondary electrons emerge is of the order of a few tens of Angstroms when the target is electrically conducting.

Accuracy - The accuracy of the system should be better than 20%. This should be sufficient to determine the relative contribution of dose enhancement to the response of MOS devices.

Precision - Accuracy could be improved by making a large number of measurements and then taking the average value. We would prefer a system with sufficient precision to obtain an accurate measurement with a single observation.

B.2.2 Constraints.

The above characteristics must be achieved within certain constraints. The essential factors are described here:

Dimensions - The dimensions will be determined by the space available in the ARACOR machine. This has a significant impact on the sensitivity of the detector.

Ease of Application - Set up and read out time should be minimal. However, unlike the ionization chamber for gamma ray induced dose enhancement, it is not expected that this will be used for regular routine measurement.

Dose Rate Limitation - It is expected that for the range of dose rates encountered with the ARACOR tester, no saturation limitations will arise.

Materials - Care will have to be used in selecting materials to simulate the targets of interest. This is due to the fact that secondary electron emission can be very sensitive to the formation of oxide and/or chemical films on the emitting surface. Available information is expected to be sufficient to avoid possible difficulties in this area.

Costs - Significant quantities of expensive materials or complex processing steps are to be avoided.

B.3 CHAMBER DESIGN FOR X-RAYS.

B.3.1 General.

Of the three approaches to the measurement of dose enhancement by x-rays, the secondary emission chamber comes closest to meeting the criteria outlined above. Our initial estimate of its performance capability, indicates the emission currents generated should range from nanoamps to picoamps depending upon the operating level of the source.

B.3.2 Design.

The overall chamber design will resemble the ionization chamber used for gamma ray dose enhancement. One major difference will be the necessity to maintain a vacuum level necessary to insure that ionization does not interfere with the measurement indicates there should not be any problem. At the low X-ray energies encountered here, the thickness of wall materials necessary to establish equilibrium is about one micrometer or less. They would not be thick enough to sustain the vacuum. For this application beryllium would probably be a suitable material since it is used in a similar application in X-ray tubes.

B.3.3 Calibration.

In order to obtain an accurate estimate of the dose enhancement factor relative or absolute measurements of the emission yield will be necessary. In making relative measurements, the response of a mixed wall chamber where both walls are the same in a manner analogous to that used in the air ionization case. However, a dual chamber such as that used for cobalt-60 will not be appropriate because of strong absorption of the primary radiation. Relative measurements in the case of X-rays would require two separate chambers.

In some cases an estimate of the actual dose rate at the interface of concern might be desired. A measure can be obtained by calibrating the emission yield against ionization. This techniques was used originally to measure the emission yields of a number of different elements [63]. It was shown in [63] that the secondary emission current I_s characteristic of the irradiated material times the dose rate D in rads per second

$$I_s = 10^{-11} Y_s D \qquad \text{(B.1)}$$

In the expression above the yield factor Y_s, is in units of reciprocal stopping power i.e., g/MeV-cm$_2$. The yield constant can be determined by measuring air ionization in the same chamber used for the emission measurements. The expression from [62] is

$$Y_s = 10^6 d\ t\ I_B/I_A\ w\ s_m \qquad \text{(B.2)}$$

where I_E and I_A are the emission and air ionization currents, d the air density in g/cm_3, t the thickness of air in the cavity in cm, w the energy required to produce an ion pair in eV, and s_m the relative mass stopping power for the cavity. All of these quantities can be readily determined.

APPENDIX C

BIBLIOGRAPHY

ADA77
A. F. Adadurov and V. T. Lazurik
Distribution of Absorbed Energy in a Layered Target Irradiated with Gamma Rays
Soviet Atomic Energy, 43,667-669,(1977)

AST88a
ASTM Committee E-10
Application of Ionization Chambers to Assess the Low Energy Gamma Component of Cobalt-60 Irradiators Used in Radiation-Hardness Testing of Silicon Electronic Devices
Standard E1250-88, 1988 Annual Book of ASTM Standards, Vol.12.02, ASTM, Philadelphia, 778-786,(September 1988)

AST88b
ASTM Committee E-10
Minimizing Dosimetry Errors in Radiation Hardness Testing of Silicon Electronic Devices Using Co-60 Sources
Standard E 1249-88, 1988 Annual Book of ASTM Standards, Vol.12.02, ASTM, Philadelphia, 762-777,(September 1988)

ATT86
F. H. Attix
Dose Near Interfaces Between Dissimilar Media Under Gamma Irradiation
Introduction to Radiological Physics, John Wiley & Sons, New York, 259-262,(1968)

BAR87
Gideon Barnea and Albert Ginzburg
High Energy X-Ray Film Response And The Intensifying Action of Metal Screens
IEEE Trans. Nucl. Sci.,NS-34(6),1580-1585,(December, 1987)

BEE76
B. L. Beers and V. W. Pine
Functional Expansion Technique for Monte Carlo Electron Transport Calculations
IEEE Trans. Nucl. Sci.,NS-23(6),1850-1856,(1976)

BEN87
J.M. Benedetto, H.E. Boesch, Jr., and T.R.Oldham, G.A. Brown
Measurement of Low-Energy X-Ray Dose Enhancement in MOS Devices with Metal Silicide Gates
IEEE Trans. Nucl. Sci.,NS-34(6),1540-1543,(December,1987)

BEN88
J.M. Benedetto, H.E Boesch, Jr., and F.B. McLean
Dose and Energy Dependence of Interface Trap Formation in Cobalt-60 and X-Ray Environments
IEEE Trans. Nucl. Sci.,NS-35(6),1260-1264,(1988)

BER71
M. J. Berger
Absorbed Dose Near an Interface Between Two Media
NBS Report 10 550,38-48,(March 1971)

BER75
R.A. Berger and J.L. Azarewicz
Packaging Effects on Transistor Radiation Response
IEEE Trans. Nucl. Sci.,NS-22(6),2568-2572,(December, 1975)

BEU87
D.E. Beutler, D.M. Fleetwood, W. Beezhold, D. Knott, L.J. Lorence, Jr., and B. L. Draper
Variations in Semiconductor Device Response in a Medium-Energy X-Ray Dose-Enhancing Environment
IEEE Trans. Nucl. Sci.,NS-34(6),1544-1550,(December,1987)

BRO80
D.B. Brown
Photoelectron Effects on the Dose Deposited in MOS Devices by Low Energy X-Ray Sources
IEEE Trans. Nucl. Sci.,NS-27(6),1465-1468,(December, 1980)

BRO81
D.B. Brown and C.M. Dozier
Electron-Hole Recombination in Irradiated SiO2 from a Microdosimetry Viewpoint
IEEE Trans. Nucl. Sci.,NS-28(6),4142-4144,(December, 1981)

BRO82
D.B. Brown and C.M. Dozier
Reducing Errors in Dosimetry Caused by Low Energy Components of Co-60 and Flash X-Ray Sources
IEEE Trans. Nucl. Sci.,NS-29(6),1996-1999,(December, 1982)

BRO86
D.B. Brown
The Phenomenon of Electron Rollout for Energy Deposition and Defect Generationin Irradiated MOS Devices
IEEE Trans. Nucl. Sci.,NS-33(6),1240-1244,(1986)

BUR71a
E. A. Burke, J. R. Cappelli, L. F. Lowe, and J. A. Wall
Solar Cell Radiation Response Near the Interface of Different Atomic Number Materials
AFCRL-72-0045,15,(24 November 1971)

BUR71b
E. A. Burke, A. R. Frederickson, J. C. Garth and J. A. Wall
Secondary Electron Phenomenology
Annual Technical Report, DNA Subtask TA040,21,(May 1971)

BUR73
T. E. Burlin, J. M. Sidwell, and B. M. Wheatley
Application of Monte Carlo Methods in Medical Radiology
Brit. J. Radiology, 46,398-399,(1973)

BUR75
E.A. Burke
Ionizing Events in Small Device Structures
IEEE Trans. Nucl. Sci.,NS-22(6),2543-2548,(December, 1975)

BUR76
E. A. Burke and J. C. Garth
An Algorithm for Energy Deposition at Interfaces
IEEE Trans. Nucl Sci., NS-23(6),1838-1843,(1976)

BUR79
E. A. Burke and J. C. Garth
Energy Deposition by Soft X-Rays - An Application to Lithography for VLSI
IEEE Trans. Nucl. Sci., NS-26(6),4868-4873,(1979)

BUR87
E.A. Burke and G.P. Summers
Extreme Damage Events Produced By Single Particles
IEEE Trans. Nucl. Sci.,NS-34(6),1575-1579,(December, 1987)

BUR89
E. A. Burke, L. F. Lowe, D. P. Snowden, J. R. Cappelli, and S. Mittleman
The Direct Measurement of Dose Enhancement in Gamma Test Facilities
IEEE Trans. Nucl. Sci.,NS-36(6),(1989)

CHA73
W. L. Chadsey
Monte Carlo Analysis of X-Ray and Gamma Ray Transition Zone Dose and Photo-Compton Current
AFCRL-TR-73-0572,50,(November 1973)

CHA74
W. L. Chadsey
X-Ray Produced Charge Deposition and Dose in Dielectrics Near Interfaces Including Space-Charge Field and Conductivity Effects
IEEE Trans. Nucl. Sci.,NS-21(6),235-242,(1974)

CHA75
W. L. Chadsey
POEM: A Fast Monte Carlo Code for the Calculation Ray Photoemission and Transition Zone Dose and Current
AFCRL-TR-75-0324,105,(January 1975)

CHA76
W. L. Chadsey, J. C. Garth, R. L. Sheppard, and R. Murphy
X-Ray Dose Enhancement Vol.I: Summary Report
RADC-TR-76-159,89,(May 1976)

CHA77
W. L. Chadsey, B. L. Beers, V. W. Pine, D. J. Srtickland, and C. W. Wilson
X-Ray Photoemission; X-Ray Dose Enhancement
RADC-TR-77-253,182,(July 1977)

CHA78a
W. L. Chadsey
X-Ray Dose Enhancement
IEEE Trans. Nucl. Sci., NS-25(6),1591-1597,(1978)

CHA78b
W. L. Chadsey
X-Ray Dose Enhancement, II
RADC-TR-78-249,64,(November 1978)

DAR79
P. J. Darley
Interface Dosimetry
Brit. J. Radiol., 52,421,(1979)

DAW81
W. R. Dawes, Jr.
An IC Compatible Ionizing Radiation Detector
IEEE Trans. Nucl. Sci., NS-28(6),4152-4155,(1981)

DEL74
T. A. Dellin, K. W. Dolan and C. J. MacCallum
Photo-Compton Currents at Material Interfaces: Theory and Experiment
IEEE Trans. Nucl. Sci., NS-21(6),227-234,(1974)

DEL76
T. A. Dellin and C. J. MacCallum
Analytical Photo-Compton Deposition Profiles
IEEE Trans. Nucl. Sci., NS-23(6),1844-1849,(1976)

DOL69
K. W. Dolan and J. L. Wirth
Non-Local Energy Deposition in Silicon by Energetic Photons
IEEE Annual Nuclear and Space Radiation Effects Conference, Summaries of Papers,215-217,(July 1969)

DOZ80
C.M. Dozier and D.B. Brown
Photon Energy Dependence of Radiation Effects in MOS Structures
IEEE Trans. Nucl. Sci.,NS-27(6),1694-1699,(1980)

DOZ81
C.M. Dozier and D.B. Brown
Effect of Photon Energy on the Response of MOS Devices
IEEE Trans. Nucl. Sci.,NS-28(6),4137-4141,(December, 1981)

DOZ83
C.M. Dozier and D.B. Brown
The Use of Low Energy X-Rays for Device Testing - A Comparison with Co-60 Radiation
IEEE Trans. Nucl. Sci.,NS-30(6),4382-4387,(December, 1983)

DOZ84
C.M. Dozier and D.B. Brown
Production of a "Standard" Radiation Environment to Minimize Dosimetry Errors in Flash X-Ray Parts Testing
IEEE Trans. Nucl. Sci.,NS-31(6),1084-1088,(December, 1984)

DOZ87
C.M.Dozier. D.M.Fleetwood, D.B.Brown, and P.S. Winokur
An Evaluation Of Low-Energy X-Ray And Cobalt-60 Irradiations Of Dos Transistors
IEEE Trans. Nucl. Sci.,NS-34,1535-1539,(December,1987)

DRE68
G. Drexler
Verlauf der Ionendosis an Grenzschichten
Proceedings of the Symposium on Microdosimetry, Published by the European Communities, Brussels,433-446,(January 1968)

DUT62
J. Dutreix, A. Dutreix et M. Bernard
Etude de la Dose au Voisinage de l'Interface entre deux Milieux de Composition Atomique Different exposes aux Rayonnement gamma du Co-60
Phys. Med. Biol., 7,69-82,(1962)

DUT64
J. Dutreix, A. Dutreix, M. Bernard, et A. Bethencourt
Etude de la Dose au Voisinage de l'Interface entre deux Milieux de Composition Atomique Different exposes aux a des RX de 11 a 20 MV
Annales de Radiologie, 7,233-241,(1964)

DUT65a
J. Dutreix et M. Bernard
Etude de Flux des Electrons Secondaires et de leur Retrodiffusion
Biophysik, 2,179-192,(1965)

DUT65b
J. Dutreix, M. Bernard
Dosimetrie au Voisinage des Interfaces dans l'Experimentation
Radiobiologique avec des rayonnements X et c de Haute Energie
Int. J. Rad. Biol., 10, 177-181

DUT65c
J. Dutreix, A. Dutreix, and M. Tubiana
Electronic Equilibrium and Transition Stages
Phys. Med. Biol., 10, 177-190

DUT66a
J. Dutreix and M. Bernard
Dosimetry at Interfaces for High Energy X and Gamma Rays
Brit. J. Radiol. 39,205-210,(1966)

DUT66b
Dutreix et M. Bernard
Dosimetrie au Voisinage des Interfaces dans l'Experimentation
Radiobiologique avec des Rayonnements X et Gamma de Haute Energie
Int. J. Rad. Biol.,10,177(1966)

DUT68
J. Dutreix and M. Bernard
Influence d'une Lame Metallique sur la Distribution de la Dose
dans le Plexiglas irradie par des Electrons de Haute Energie
Biophyik,4,302-310,(1968)

EIS71
H. Eisen
Electron Depth-Dose Distribution Measurements in Metals and
Two-Layer Slabs
Ph.D. Thesis, University of Maryland,,(1971)

EIS72a
H. Eisen, M. Rosenstein, and J. Silverman
2.00-MeV Electron Depth-Dose Measurements in Aluminum, Copper and
Tin Absorbers Using a Radiochromic Dye Film
Int. J. Appl. Rad. and Isotopes,23,97-108,(1972)

EIS72b
H. Eisen, M. Rosenstein and J. Silverman
Electron Depth-Dose Distribution Measurements in Two-Layer Slab
Absorbers
Radiat. Res., 52,420-447,(1972)

EME73
L. C. Emerson, R. D. Birkhoff, V. E. Anderson, and R. H. Ritchie
Electron Slowing Down Spectrum in Irradiated Silicon
Phys. Rev. B, 7,1798-1811,(1973)

FLE85
D.M. Fleetwood, P.S. Winokur, R.W. Beegle, P.V. Dressendorfer and
B.L. Draper
Accounting for Dose-Enhancement Effects with CMOS Transistors
IEEE Trans. Nucl. Sci.,NS-32(6),4369-4375,(December, 1985)

FLE85
D.M. Fleetwood, P.S. Winokur, R.W. Beegle, P. V. Dressendorfer,
and B. L. Draper
Accounting for Dose-Enhancement Effects with CMOS Transistors
IEEE Trans. Nucl. Sci.,NS-32(6),4369-4375,(1985)

FLE86
D. M. Fleetwood, P.S. Winokur, L.J. Lorence Jr.,W. Beezhold, P.
V. Dressendorfer,and J.R. Schwank
The Response of MOS Devices to Dose-Enhanced Low Energy-Radiation
IEEE Trans. Nucl. Sci.,NS-33(6),1245-1251,(1986)

FLE88
D.M. Fleetwood, D.E. Beutler, L.J. Lorence Jr., D.B. Brown, B.L.
Draper, L.C. Riewe, H.B. Rosenstock, and D. P. Knott
Comparison of Enhanced Device Response and Predicted X-Ray Dose
Enhancement Effects on MOS Oxides
IEEE Trans. Nucl. Sci.,NS-35(6),1265-1271,(1988)

FRE71
A. R. Frederickson and E. A. Burke
Ionization, Secondary Emission, and Compton Currents at Gamma
Irradiated Interfaces
IEEE Trans. Nucl. Sci., NS-18(6),162-169,(1971)

FRE72
A. R. Frederickson and E. A. Burke
Ionization, Secondary Emission, and Compton Currents at Gamma
Irradiated Interfaces
IEEE Trans. Nucl. Sci., NS-18(6),162-169,(1972)

FRE75
A.R. Frederickson
Charge Deposition, Photoconduction and Replacement Current in Irradiated Multilayer Structures
IEEE Trans. Nucl. Sci.,NS-22,2556-2562,(December, 1975)

FRE79
A. R. Frederickson
Gamma Energy Spectra for the RADC/ES Cobalt 60 Sources
RADC-TR-79-68,20,(April 1979)

GAR75
J.C. Garth, W.L. Chadsey and R.L. Sheppard Jr.
Monte Carlo Analysis of Dose Profiles Near Photon Irradiated Material Interfaces
IEEE Trans. Nucl. Sci.,NS-22,2562-2567,(December, 1975)

GAR78
J. C. Garth
Diffusion Equation Model for Kilovolt Electron Transport at X-Irradiated Interfaces
IEEE Trans. Nucl. Sci., NS-25(6),1598-1606,(1978)

GAR80
J.C. Garth, E.A. Burke and S. Woolf
The Role of Scattered Radiation in the Dosimetry of Small Device Structures
IEEE Trans. Nucl. Sci.,NS-27(6),1459-1464,(December, 1980)

GAR81
J.C. Garth
High Energy Extension of the Semi-Emperical Model for Energy Depositon at Interfaces
IEEE Trans. Nucl. Sci.,NS-28(6),4145-4151,(December, 1981)

GAR82
J.C. Garth, B.W. Murray and R.P. Dolan
Soft X-Ray Induced Energy Deposition in a Three-Layered System: Au/C/PBS
IEEE Trans. Nucl. Sci.,NS-29(6),1985-1991,(December, 1982)

GAR85
J.C. Garth, E.A. Burke and S. Woolf
Displacement Damage and Dose Enhancement in Gallium Arsenide and Silicon
IEEE Trans. Nucl. Sci.,NS-32(6),4382-4387,(December, 1985)

GAR87
J.C. Garth, S. Woolf
Comparison Of Onetran Calculations Of Electron Beam Dose Profiles
With Monte Carlo And Experiment
IEEE Trans. Nucl. Sci.,NS-34,1551-1556,(December 1987)

GAR89
J. C. Garth
Calculations of Dose Enhancement in Device Structures
Nucl. Instr. Meth.,B40/41,1266-1270,(1989)

HAM86
R.N. Hamm
Dose Calculations for Si-SiO2Si Layered Structures Irradiated by
X Rays and 60Co Gamma Rays
IEEE Trans. Nucl. Sci.,NS-33(6),1236-1239,(1986)

HAR86
R.R. Hart, W. Beezhold, L.J. Lorence Jr. and A. J. Smith
Comparison of Measured Dose Enhancement Effects in LiF TLD's with
2-D Monte Carlo Predictions
IEEE Trans. Nucl. Sci.,NS-33(6),1258-1260,(1986)

HON75
V.R. Honnold, M. Goldberg, W.A. Schreiner and A.A. Witteles
Investigation of DI and JI CMOS FXR Response at Different
Spectral Energies
IEEE Trans. Nucl. Sci.,NS-22(6),2650-2655,(December, 1975)

HOR83
Y. S. Horowitz, M. Moscovitch, and A. Dubi
Modified General Cavity Theory Applied to the Calculation of
Gamma Dose in Co-60 Thermoluminescence Dosimetry
Phys. Med. Biol., 28,829-840,(1983)

HOR86
Y. S. Horowitz, M. Moscovitch, J. M. Mack, H. Hsu and E. Kearsley
Incorporation of Monte Carlo Electron Interface Studies into
Photon General Cavity Theory
Nucl. Sci. Eng., 94,233-240,(1986)

KEA84
E. Kearsley
A New General Cavity Theory
Phys. Med. Biol., 29,1179-1187,(1984)

KEL83
J.G. Kelly, T.F. Luera, L.D. Posey, D.W. Vehar, D.B. Brown and C.M. Dozier
Dose Enhancement Effects in MOSFET IC's Exposed in Typical Co-60 Facilities
IEEE Trans. Nucl. Sci.,NS-30(6),4388-4393,(December, 1983)

KER85
K. G. Kerris and S. G. Gorbics
Experimental Determination of the Low Energy Spectral Component of Cobalt-60 Sources
IEEE Trans. Nucl. Sci., NS-32(6),4356-4362,((1985))

KER86
K. G. Kerris and S. G. Gorbics
Experimental Determination of the Low-Energy Spectral Component of Cobalt-60 Sources
HDL-TR-2082,37,(April 1986)

KER87
K. G. Kerris
The Theory and Practice of Radiation Dosimetry in the Radiation Hardness Testingof Electronic Devices and Systems
HDL-TR-2107,33,(April 1987)

KER89
K. G. Kerris
Source Considerations and Testing Techniques
Ionizing Radiation Effects in MOS Devices and Circuits, T. P. Ma and P. V. Dressendorfer, Eds.,John Wiley & Sons, New York, 443-484,(1989)

KRO74
S. Kronenberg, R. Lux, K. Nilson, G. Jurczyk, R. Pfeffer, and H. Berkowitz
Gamma Induced Charge Buildup in Insulators
IEEE Trans. Nucl. Sci., NS-21(6),243-248,(1974)

LAN74
J. B. Langworthy, M. Rosen, F. H. Attix, S. G. Gorbics, and S. M. Seltzer
Dose Perturbations at X-Ray Irradiated Interfaces
Trans. Am. Nucl. Soc., 19,453,(1974)

LOC76
G. J. Lockwood, G. H. Miller and J. A. Halbleib
Electron Energy Deposition in Multilayer Geometries
IEEE Trans. Nucl. Sci.,NS-23(6),1862-1866,(1976)

LON74
D. M. Long and D. H. Swant
Dose Gradient Effects on Semiconductors
AFCRL-TR-74-0283,99,(July 1974)

LON82
D.M. Long, D.G. Millward and J. Wallace
Dose Enhancement Effects in Semiconductor Devices
IEEE Trans. Nucl. Sci.,NS-29(6),1980-1984,(December, 1982)

LON83
D. M. Long, D. G. Millward, R. L. Fitzwilson, and W. L. Chadsey
Handbook for Dose Enhancement Effects in Electronic Devices
RADC-TR-83-84,,(March 1983)

LOW75
L. F. Lowe, W. C. Taylor and J. R. Cappelli
Interface Dose as a Function of Angle of Incidence for
Aluminum-Gold and Aluminum-Beryllium Slabs
AFCRL-TR-75-0206,9,(11 April 1975)

LOW78a
D. Lowe
Transition Zone Dosimetry and its Application to Reactor Shield
Surveys
J. Inst. Nuc. Eng., 19(6),191-194,(1978)

LOW78b
D. Lowe
Interface Dosimetry
Brit. J. Radiology, 51,60,(1978)

LOW82
L.F. Lowe, J.R. Cappelli and E.A. Burke
Dosimetry Errors in Co-60 Gamma Cells Due to Transition Zone
Phenomena
IEEE Trans. Nucl. Sci.,NS-29(6),1992-1995,(December, 1982)

LUR75
N.A. Lurie, L.Harris,Jr., D.K. Steinman, J.C. Young, S.J. Fiesehahn, and J. P. Wondra
Neutron-Induced Dose Enhancement in Tantalum
IEEE Trans. Nuc. Sci.,NS-22(6),2573-2575,(1975)

MCL85
W. L. McLaughlin, J. C. Humphreys, M. Farahani, A. Miller
Measurement of High Doses Near Metal and Ceramic Interfaces
High Dose Dosimetry Proceedings of an International Symposium on High Dose Dosimetry,IEAE,109-133,(1985)

MEU87C
A. Meulenberg, C.M. Dozier, W. T. Andersen, S.D. Mittleman, M.H. Zugich, and C.E. Caefer
Dosimetry and Total Dose Radiation Testing of GaAs Devices
IEEE Trans. Nucl. Sci.,NS-34(6),1745-1750,(1987)

MIL85
D.G. Millward, and M. Merker
Time Dependent Dose Enhancement Effects in Integrated Circuit Transient Response Mechanisms
IEEE Trans. Nucl. Sci.,NS-32(6),4376-4381,(December, 1985)

MIL85
D.G. Milward and M. Merker
Time Dependent Dose Enhancement Effects on Integrated Circuit Transient Response Mechanisms
IEEE Trans. Nucl. Sci.,NS-32(6),4376-4381,(1985)

MIM69
L. S. Mims and R. A. Williams
Effects of Packaging on Radiation-Induced Responses
IEEE Annual Nuclear and Space Radiation Effects Conference, Summaries of Papers,219-222,(July 1969)

NAH88
A. E. Nahum
Simulation of Dosimeter Response and Interface Effects
Monte Carlo Transport of Electrons and Photons, T.M. Jenkins, W. R. Nelson, and A. Rindi, Eds., Plenum Press, New York,523-547,(1988)

OGU80
O. T. Ogunleye, F. H. Attix and B. R. Paliwal
Comparison of Burlin Cavity Theory with LiF TLD Measurements for Cobalt-60 Gaamma Rays
Phys. Med. Biol., 25,203-213,(1980)

OLD83
T.R. Oldham and J.M. McGarrity
Comparison of Cobalt-60 Response and 10 keV X-Ray Response in MOS Capacitors
IEEE Trans. Nucl. Sci.,NS-30(6),4377-4381,(December, 1983)

PAL84
L. J. Palkuti
Comprehensive Radiation Testing of ICs at the Wafer Stage
Presented at the IEEE 1984 Annual Conference on Nuclear and Space Radiation Effects,16,(July 1984)

PIG76
J. Pigneret and H. Stroback
Electrical Response of Irradiated Multilayer Structures
IEEE Trans. Nucl. Sci., NS-23(6),1886-1896 ,(1976)

POS85
L.D. Posey. T.F. Wrobel, D.C. Evans, W. Beezhold, J.G. Kelly, C.J. MacCallum, F.N. Coppage. T.F. Luera, L.J. Lorence and A.J. Smith
MOS-Transistor Radiation Detectors and X-Ray Dose-Enhancement Effects
IEEE Trans. Nucl. Sci.,NS-32(6),4446-4452,(December, 1985)

PRE85
A. L. Pregenzer and J. A. Halbleib
Accuracy of Coupled Monte-Carlo/Next-Event-Estimator for Bremsstrahlung Dose Predictions
IEEE Trans. Nucl. Sci.,NS-32(6),4405-4409,(December, 1985)

SEL87
S. M. Seltzer and M. J. Berger
Energy Deposition by Electron Bremsstrahlung, and Co-60 Gamma-Ray Beams in Multi-Layer Media
Int. J. Appl. Radiat. and Isotopes, 38,349-364,(1987)

SPI51
F. W. Spiers
Dosage in Irradiated Soft Tissue and Bone
Brit. J. Radiology, 24, 365-370 (1951)

SPI69
F. W. Spiers
Transition-Zone Dosimetry
Radiation Dosimetry, 2nd ed., Vol.3, F. H. Attix and E. Tochilin, Eds., Academic Press, New York,809-867,(1969)

TUN76
C. J. Tung, J. C. Ashley, V. E. anderson and R, H, Ritchie
Inverse Mean Free Path, Stopping Power, CSDA Range, and Straggling in Silicon and Silicon Dioxide for Electrons of Energy < 10 keV
RADC-TR-76-125,58,(April 1976)

TUN83
C.J. Tung and C.P. Wang
Multiple Scattering of Low Energy Electrons in Aluminum
IEEE Trans. Nucl. Sci.,NS-30(6),4409-4412,(December, 1983)

UNN79
K. Unnikrishnan and V. Sundararaman
Dose Distribution Near an Interface Due to Anisotropic Electron Emission
Radiat. Res.,77,201-208,(1979)

WAL70
J.A. Wall and E.A. Burke
Gamma Dose Distributions at and Near the Interface of Different Materials
IEEE Trans. Nucl. Sci.,NS-17(6),305-309,(December (1970)

WAL74
J. A. Wall and E. A. Burke
Dose Distributions At and Near the Interface of Different Materials Exposed to Cobalt-60 Gamma Radiation
AFCRL-TR-75-0004,29,(17 December 1974)

WEB79
S. Webb
The Absorbed Dose in the Vicinity of an Interface Between Two Media Irradiated by a Co-60 Source
Brit. J. Radiology, 52,962-967,(1979)

WIN62
C. L. Wingate, W. Gross, and G. Failla
Experimental Determination of Absorbed Dose from X-Rays Near the Interface of Soft Tissue and Other Material
Radiology,79,984-1000,(1962)

WOO83
S. Woolf and A.R. Frederickson
Photon Spectra in Cobalt-60 Gamma Test Cells
IEEE Trans. Nucl. Sci., NS-30(6),4371-4376,(December, 1983)

WOO84
S. Woolf and E.A. Burke
Monte Carlo Calculations of Irradiation Test Photon Spectra
IEEE Trans. Nucl. Sci.,NS-31(6),1089-1094,(1984)

WOO86
S. Woolf and J. C. Garth
Comparison of Onetran Calculations with Cobalt-60 Dose Profile
Data to Determine the Photon Spectrum
IEEE Trans. Nucl. Sci.,NS-33(6),1252-1257,(1986)

DISTRIBUTION LIST

DNA-TR-89-273

DEPARTMENT OF DEFENSE

ASSISTANT TO THE SECRETARY OF DEFENSE
ATTN: EXECUTIVE ASSISTANT

DEFENSE ADVANCED RSCH PROJ AGENCY
ATTN: ASST DIR (ELECTRONIC SCIENCES DIV)
ATTN: R REYNOLDS

DEFENSE ELECTRONIC SUPPLY CENTER
ATTN: DESC-E

DEFENSE INTELLIGENCE AGENCY
ATTN: DT-1B
ATTN: RTS-2B

DEFENSE NUCLEAR AGENCY
ATTN: RAEE (TREE)
2 CYS ATTN: TITL

DEFENSE NUCLEAR AGENCY
ATTN: TDNM
2 CYS ATTN: TDTT W SUMMA

DEFENSE TECHNICAL INFORMATION CENTER
2 CYS ATTN: DTIC/FDAB

DNA PACOM LIAISON OFFICE
ATTN: DNALO

FIELD COMMAND DEFENSE NUCLEAR AGENCY
ATTN: FCPF R ROBINSON

JOINT DATA SYSTEM SUPPORT CTR
ATTN: C-330
ATTN: JNSV

STRATEGIC AND THEATER NUCLEAR FORCES
ATTN: DR E SEVIN

THE JOINT STAFF
ATTN: JKC (ATTN: DNA REP)
ATTN: JKCS
ATTN: JPEM

DEPARTMENT OF THE ARMY

HARRY DIAMOND LABORATORIES
ATTN: SLCHD-NW-RP
ATTN: SLCHD-NW-TS

INFORMATION SYSTEMS COMMAND
ATTN: STEWS-NE-AN J MEASON

U S ARMY GARRISON
ATTN: LIBRARY BLDG 80112

U S ARMY MISSILE COMMAND
ATTN: AMCPM-HA-SE-MS

U S ARMY MISSILE COMMAND/AMSMI-RD-CS-R
ATTN: AMSMI-RD-CS-R (DOCS)

U S ARMY NUCLEAR & CHEMICAL AGENCY
ATTN: MONA-NU (D. BASH)

U S ARMY RESEARCH OFFICE
ATTN: R GRIFFITH

U S ARMY STRATEGIC DEFENSE CMD
ATTN: CSSD-H-SAV
ATTN: CSSD-SD-A

U S ARMY STRATEGIC DEFENSE COMMAND
ATTN: CSSD-SL

DEPARTMENT OF THE NAVY

NAVAL AIR SYSTEMS COMMAND
ATTN: AIR-530TC

NAVAL ELECTRONICS ENGRG ACTVY, PACIFIC
ATTN: CODE 250

NAVAL POSTGRADUATE SCHOOL
ATTN: CODE 1424 LIBRARY

NAVAL RESEARCH LABORATORY
ATTN: CODE 4611 E PETERSON
ATTN: CODE 4653 A NAMENSON
ATTN: CODE 4682 C DOZIER
ATTN: CODE 4682 D BROWN
ATTN: CODE 6813 N SAKS
ATTN: CODE 6816 E D RICHMOND
ATTN: CODE 6816 H HUGHES

NAVAL SURFACE WARFARE CENTER
ATTN: F WARNOCK
ATTN: R SMITH

NAVAL SURFACE WARFARE CENTER
ATTN: CODE H-21

NAVAL TECHNICAL INTELLIGENCE CTR
ATTN: LIBRARY

NAVAL WEAPONS EVALUATION FACILITY
ATTN: CLASSIFIED LIBRARY

NAVAL WEAPONS SUPPORT CENTER
ATTN: D PLATTETER

DEPARTMENT OF THE AIR FORCE

AERONAUTICAL SYSTEMS DIVISION
ATTN: ASD/ENSS

AIR FORCE CTR FOR STUDIES & ANALYSIS
ATTN: AFCSA/SAMI (R GRIFFIN)

AIR UNIVERSITY LIBRARY
ATTN: AUL LSE

OGDEN AIR LOGISTICS CENTER
ATTN: OO-ALC/MMDEC/HARDNESS CONTROL
ATTN: OO-ALC/MMGR/DOCUMENT CONTROL

PHILLIPS LABORATORY
ATTN: AFSTC/CA/MAJ HUNT
ATTN: NTCA
ATTN: NTCAS
ATTN: NTCER R MAIER

ROME AIR DEVELOPMENT CENTER, AFSC
ATTN: RBR J BRAUER

ROME AIR DEVELOPMENT CENTER, AFSC
ATTN: ESR

SPACE DIVISION/YA
ATTN: YAS

SPACE DIVISION/YAR
ATTN: YAR CAPT STAPANIAN

SPACE DIVISION/YD
ATTN: YD

STRATEGIC AIR COMMAND/XRFS
ATTN: XRFS

WRIGHT RESEARCH & DEVELOPMENT CENTER
ATTN: AFWAL/ELE
ATTN: WRDC/MTE

3416TH TECHNICAL TRAINING SQUADRON (ATC)
ATTN: TTV

DEPARTMENT OF ENERGY

ALBUQUERQUE OPERATIONS OFFICE
ATTN: NESD

LAWRENCE LIVERMORE NATIONAL LAB
ATTN: J YEE
ATTN: H KRUGER
ATTN: W ORVIS

LOS ALAMOS NATIONAL LABORATORY
ATTN: E LEONARD

SANDIA NATIONAL LABORATORIES
ATTN: DR T F WROBEL, DIV 9342
ATTN: ORG 2144 P V DRESSENDORFER
ATTN: ORG 2146 T A DELLIN

OTHER GOVERNMENT

CENTRAL INTELLIGENCE AGENCY
ATTN: OSWR/NED
ATTN: OSWR/STD/MTB

DEPARTMENT OF TRANSPORTATION
ATTN: ARD 350

NASA
ATTN: DR JAMES TRAINOR
ATTN: V DANCHENKO
ATTN: M JHABVALA

NATIONAL INSTITUTE OF STANDARDS & TECHNOLOGY
ATTN: P ROITMAN

DEPARTMENT OF DEFENSE CONTRACTORS

ADVANCED RESEARCH & APPLICATIONS CORP
ATTN: R ARMISTEAD

AEROSPACE CORP
ATTN: A AMRAM
ATTN: K G HOLDEN
ATTN: M HOPKINS
ATTN: P BUCHMAN
ATTN: W A KOLASINSKI

ALLIED-SIGNAL, INC
ATTN: DOCUMENT CONTROL

AMPEX CORP
ATTN: B RICKARD
ATTN: K WRIGHT

ANALYTIC SERVICES, INC (ANSER)
ATTN: A HERNDON
ATTN: A SHOSTAK

BDM INTERNATIONAL INC
ATTN: D WUNSCH

BOEING CO
ATTN: A JOHNSTON
ATTN: M ANAYA
ATTN: I ARIMURA

BOOZ-ALLEN & HAMILTON, INC
ATTN: D VINCENT
ATTN: L ALBRIGHT

CALIFORNIA INSTITUTE OF TECHNOLOGY
ATTN: C BARNES

CALSPAN CORP
ATTN: R THOMPSON

CHARLES STARK DRAPER LAB, INC
ATTN: N TIBBETTS

CINCINNATI ELECTRONICS CORP
ATTN: L HAMMOND

CLEMSON UNIVERSITY
ATTN: P J MCNULTY

COMPUTER SCIENCES CORP
ATTN: A SCHIFF

DAVID SARNOFF RESEARCH CENTER, INC
ATTN: R SMELTZER

E-SYSTEMS, INC
ATTN: K REIS

EATON CORP
ATTN: R BRYANT

ELECTRONIC INDUSTRIES ASSOCIATION
ATTN: J KINN

FORD AEROSPACE CORPORATION
ATTN: TECHNICAL LIBRARY

GENERAL ELECTRIC CO
ATTN: DOCUMENTS LIBRARY
ATTN: J ANDREWS
ATTN: TECHNICAL LIBRARY

GENERAL ELECTRIC CO
ATTN: B FLAHERTY
ATTN: L HAUGE

GENERAL ELECTRIC CO
ATTN: G GATI MD

GENERAL ELECTRIC CO
ATTN: DAREN NERAD

GENERAL ELECTRIC CO
ATTN: J MILLER

GENERAL RESEARCH CORP
ATTN: A HUNT

GEORGE WASHINGTON UNIVERSITY
ATTN: A FRIEDMAN

GRUMMAN AEROSPACE CORP
ATTN: J ROGERS

H. M. WEIL CONSULTANTS, INC
ATTN: H WEIL

HARRIS CORP
ATTN: J C LEE
ATTN: J W SWONGER

HARRIS CORPORATION
ATTN: E YOST
ATTN: W ABARE

HONEYWELL INC
ATTN: R JULKOWSKI

HONEYWELL SYSTEMS & RESEARCH CENTER
ATTN: R BELT

HONEYWELL, INC
ATTN: MS 725 5

HUGHES AIRCRAFT CO
ATTN: SYSTEMS TECH DEPT /W SCHENET

HUGHES AIRCRAFT COMPANY
ATTN: E KUBO
ATTN: L DARDA

IBM CORP
ATTN: DEPT L75,

IBM CORP
ATTN: J ZIEGLER

IBM CORP
ATTN: N HADDAD

IIT RESEARCH INSTITUTE
ATTN: I MINDEL

INSTITUTE FOR DEFENSE ANALYSES
ATTN: TECH INFO SERVICES

JAYCOR
ATTN: R STAHL

JAYCOR
ATTN: R SULLIVAN

JAYCOR
ATTN: R POLL

JOHNS HOPKINS UNIVERSITY
ATTN: R MAURER

KAMAN SCIENCES CORP
ATTN: B KINSLOW

KAMAN SCIENCES CORP
ATTN: DASIAC

KAMAN SCIENCES CORPORATION
ATTN: DASIAC

KEARFOTT GUIDANCE AND NAVIGATION CORP
ATTN: J D BRINKMAN

LITTON SYSTEMS INC
ATTN: F MOTTER
ATTN: S MACKEY

LOCKHEED MISSILES & SPACE CO, INC
ATTN: TECHNICAL INFORMATIION CENTER

LOCKHEED MISSILES & SPACE CO, INC
ATTN: B KIMURA

LOCKHEED SANDERS, INC
ATTN: BRIAN G CARRIGG

LTV AEROSPACE & DEFENSE COMPANY
2 CYS ATTN: LIBRARY EM-08

MARTIN MARIETTA CORP
ATTN TIC/MP 30

MARTIN MARIETTA CORP
ATTN S BUCHNER

MARTIN MARIETTA DENVER AEROSPACE
ATTN RESEARCH LIBRARY

MARYLAND, UNIVERSITY OF
ATTN: H C LIN

MCDONNELL DOUGLAS CORP
ATTN: A P MUNIE
ATTN: R L KLOSTER

MCDONNELL DOUGLAS CORPORATION
ATTN: P ALBRECHT

MESSENGER, GEORGE C
ATTN: G MESSENGER

MISSION RESEARCH CORP
ATTN: C LONGMIRE
2 CYS ATTN: E BURKE

MISSION RESEARCH CORP
ATTN: J LUBELL
ATTN: W WARE

MISSION RESEARCH CORP, SAN DIEGO
ATTN: J RAYMOND
ATTN: V VAN LINT

MITRE CORPORATION
ATTN: J R SPURRIER
ATTN: M FITZGERALD

MOTOROLA, INC
ATTN: COMM SECURITY OFFICE

NATIONAL SEMICONDUCTOR CORP
ATTN: F C JONES

NICHOLS RESEARCH CORP, INC
ATTN: HUGO HARDT

NORDEN SYSTEMS, INC
ATTN: TECHNICAL LIBRARY

NORTHROP CORP
ATTN: A BAHRAMAN

NORTHROP CORPORATION
ATTN: J R SROUR

PACIFIC-SIERRA RESEARCH CORP
ATTN: H BRODE

PHYSITRON INC
ATTN: MARK CHRISTOPHER

PHYSITRON INC
ATTN: MARION ROSE

R & D ASSOCIATES
ATTN: D CARLSON

RAND CORP
ATTN: C CRAIN

RAND CORP
ATTN: B BENNETT

RAYTHEON CO
ATTN: JOSEPH SURRO

RCA CORPORATION
ATTN: G BRUCKER

RESEARCH TRIANGLE INSTITUTE
ATTN: M SIMONS

ROCKWELL INTERNATIONAL CORP
ATTN: T YATES

ROCKWELL INTERNATIONAL CORP
ATTN: YIN-BUTE YU

S-CUBED
ATTN: J KNIGHTEN
ATTN: LLOYD DUNCAN

SCIENCE APPLICATIONS INTL CORP
ATTN: D MILLWARD
ATTN: DAVID LONG

SCIENCE APPLICATIONS INTL CORP
ATTN: J RETZLER

SCIENCE APPLICATIONS INTL CORP
ATTN: W CHADSEY

SCIENCE APPLICATIONS INTL CORP
ATTN: P ZIELIE

SCIENTIFIC RESEARCH ASSOC, INC
ATTN: H GRUBIN

SUNDSTRAND CORP
ATTN: C WHITE

SYSTRON-DONNER CORP
ATTN: SECURITY OFFICER

TECHNOLOGY DEVELOPMENT ASSOCIATES
ATTN: R V BENEDICT

TELEDYNE BROWN ENGINEERING
ATTN: G R EZELL
ATTN: LEWIS T SMITH

TELEDYNE SYSTEMS CO, INC
ATTN: R SUHRKE

TEXAS INSTRUMENTS, INC
ATTN: T CHEEK

TRW
ATTN: M J TAYLOR

TRW INC
ATTN: D AUSHERMAN
ATTN: M J TAYLOR
ATTN: P GUILFOYLE

TRW SPACE & DEFENSE SECTOR
ATTN: C BLASNEK
ATTN: DR D R GIBSON

TRW SPACE & DEFENSE SECTOR SPACE &
ATTN: HL DEPT/LIBRARY

UNISYS CORPORATION-DEFENSE SYSTEMS
ATTN: P MARROFFINO

VISIDYNE, INC
ATTN: C H HUMPHREY
ATTN: W P REIDY

FOREIGN

FOA 2
ATTN: B SJOHOLM

FOA 3
ATTN: T KARLSSON